ML in healthcare

Christian Salvatore
Scuola Universitaria Superiore IUSS Pavia

christian.salvatore@iusspavia.it

Genomics can predict subtypes

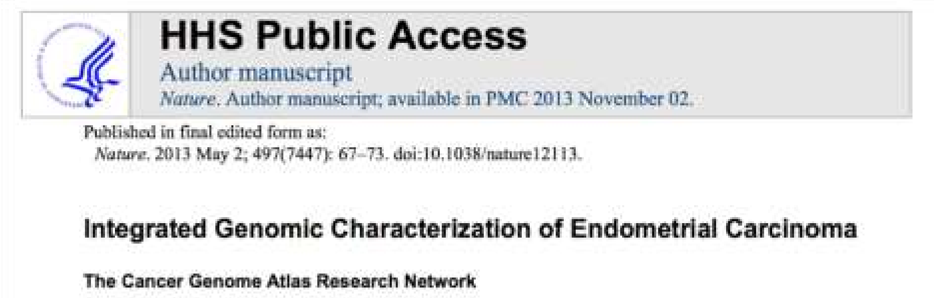
HHS Public Access
Author manuscript
Nature. Author manuscript; available in PMC 2013 November 02.

Published in final edited form as:
Nature. 2013 May 2; 497(7447): 67–73. doi:10.1038/nature12113.

Integrated Genomic Characterization of Endometrial Carcinoma

The Cancer Genome Atlas Research Network

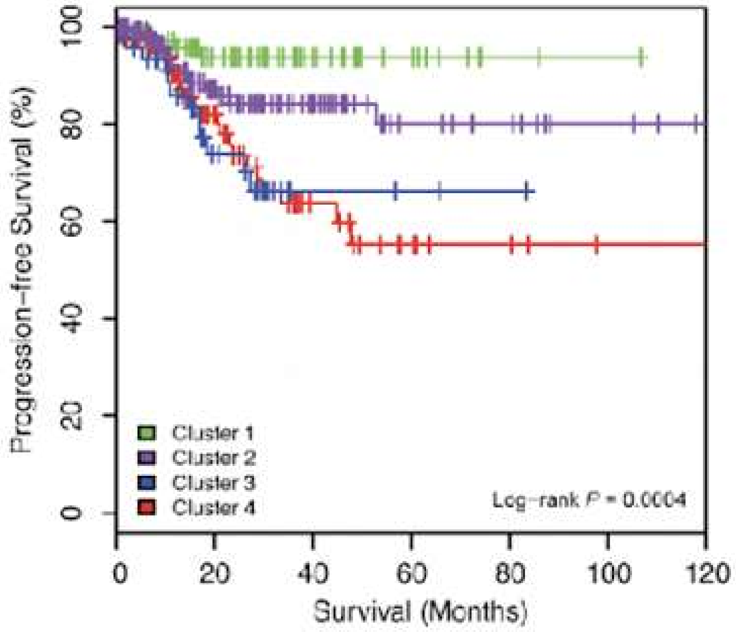

genes

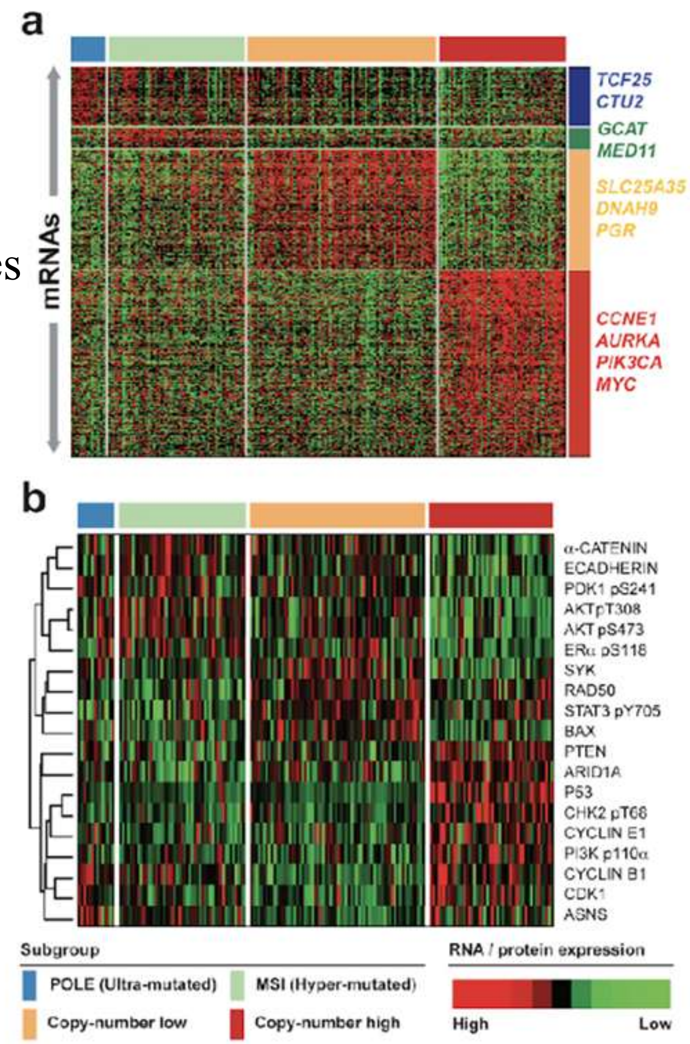

However… biopsy genomics can fail for INTER/INTRA-TUMOUR HETEROGENEITY

The NEW ENGLAND JOURNAL of MEDICINE

MARCH 8, 2012

Intratumor Heterogeneity and Branched Evolution Revealed by Multiregion Sequencing

Marco Gerlinger, M.D., Andrew J. Rowan, B.Sc., Stuart Horswell, M.Math., James Larkin, M.D., Ph.D., David Endesfelder, Dip.Math., Eva Gronroos, Ph.D., Pierre Martinez, Ph.D., Nicholas Matthews, B.Sc., Aengus Stewart, M.Sc., Patrick Tarpey, Ph.D., Ignacio Varela, Ph.D., Benjamin Phillimore, B.Sc., Sharmin Begum, M.Sc., Neil Q. McDonald, Ph.D., Adam Butler, B.Sc., David Jones, M.Sc., Keiran Raine, M.Sc., Calli Latimer, B.Sc., Claudio R. Santos, Ph.D., Mahrokh Nohadani, H.N.C., Aron C. Eklund, Ph.D., Bradley Spencer-Dene, Ph.D., Graham Clark, B.Sc., Lisa Pickering, M.D., Ph.D., Gordon Stamp, M.D., Martin Gore, M.D., Ph.D., Zoltan Szallasi, M.D., Julian Downward, Ph.D., P. Andrew Futreal, Ph.D., and Charles Swanton, M.D., Ph.D.

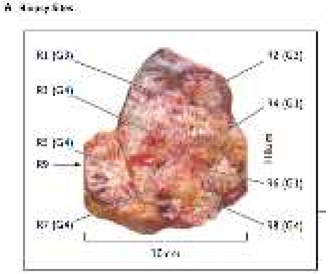

multiple spatially separated samples obtained from 4 primary renal carcinomas and associated metastatic sites

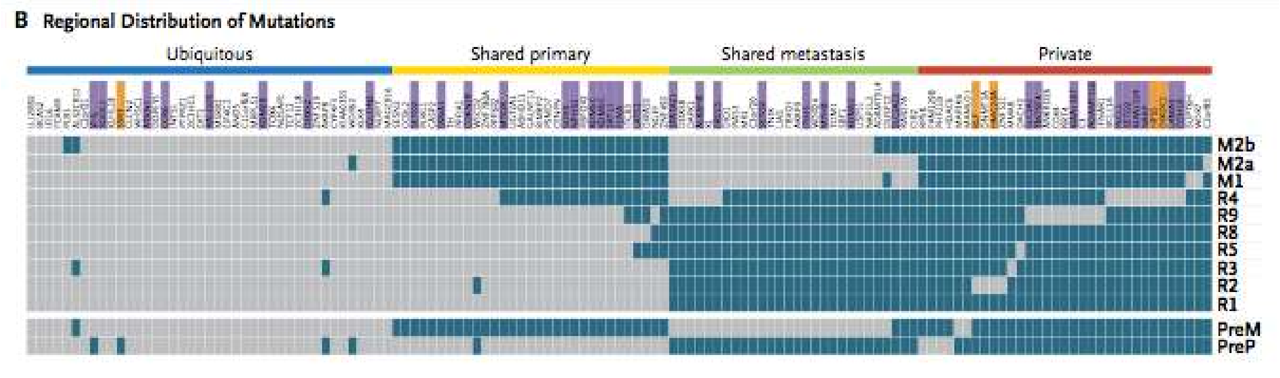

Gray = presence of a mutation
Dark blu = absence

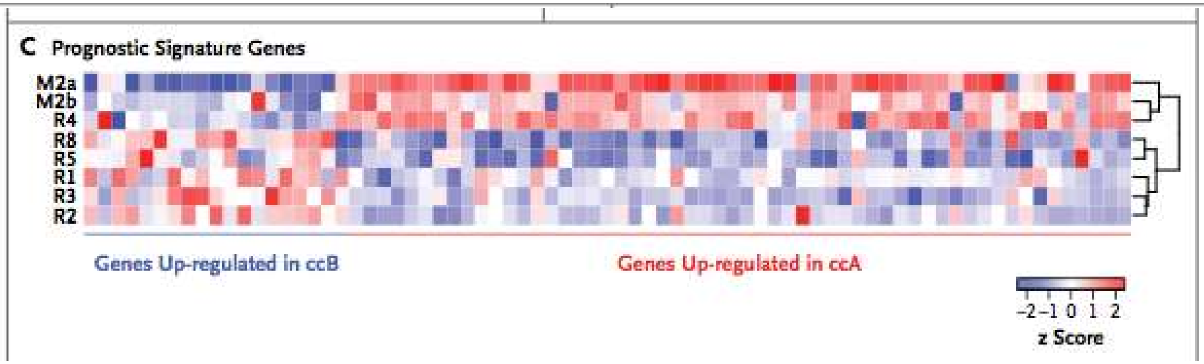

2 molecular subgroups:
clear-cell A (good prognosis)
clear-cell B (poor prognosis)

Can in vivo imaging
capture INTER/INTRA-LESION subtype heterogeneity
(US, CT, MRI, PET-CT)?

Can in vivo imaging of the lesion
be used as a digital biobank?

Image features (semantic)

a large uterine mass with nodular superior and posterior borders

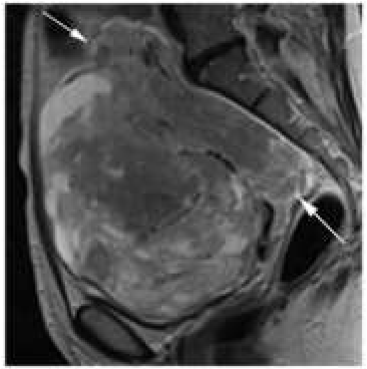

MRI T2-weighted

dark area in the myometrial mass

MRI T2-weighted

intra-lesional haemorrhage

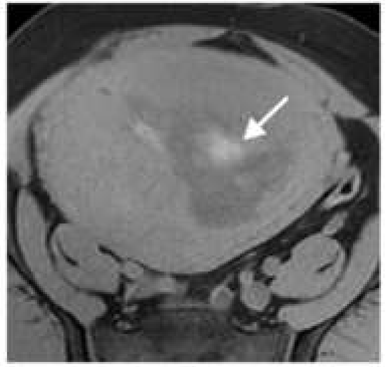

Non contrast-enhanced MRI T1-weighted fat saturated

central unenhanced areas

Contrast-enhanced MRI T1-weighted fat saturated

Image features and genomics

IF 68.84

NATURE BIOTECHNOLOGY VOLUME 25 NUMBER 6 JUNE 2007

Liver cancer

Decoding global gene expression programs in liver cancer by noninvasive imaging

Eran Segal[1], Claude B Sirlin[2], Clara Ooi[4], Adam S Adler[5], Jeremy Gollub[6], Xin Chen[8], Bryan K Chan[2], George R Matcuk[7], Christopher T Barry[3], Howard Y Chang[5] & Michael D Kuo[2]

32 CT imaging semantic features

116 gene "modules"
with coherent patterns of variations

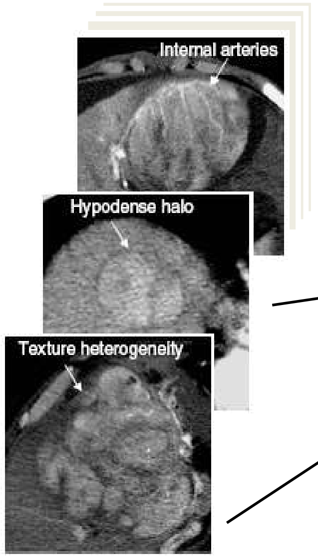

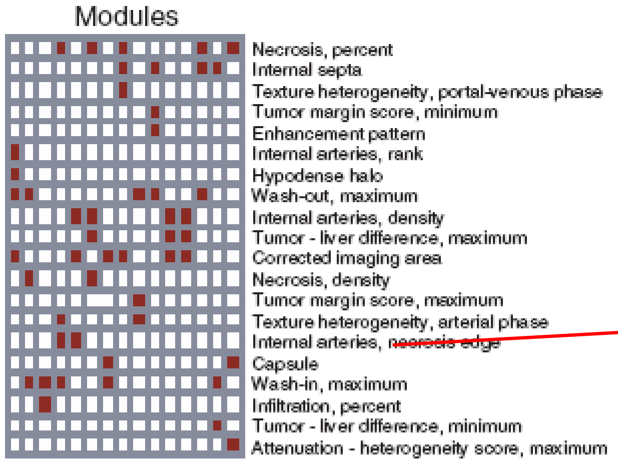

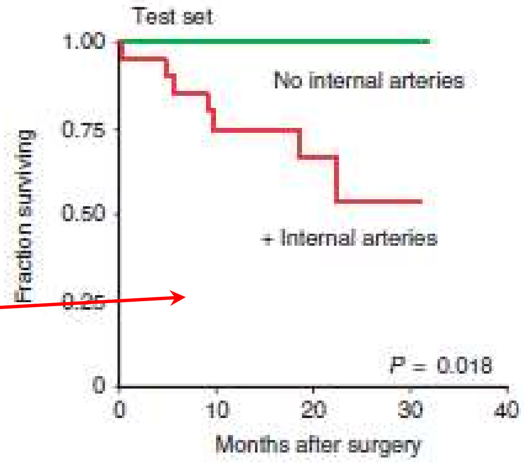

Red=presence

Green=absence

Image features and genomics

IF 11.20

PNAS | April 1, 2008 | vol. 105 | no. 13 | 5213–5218

Brain cancer

Identification of noninvasive imaging surrogates for brain tumor gene-expression modules

Maximilian Diehn*†, Christine Nardini*, David S. Wang*, Susan McGovern‡, Mahesh Jayaraman§, Yu Liang¶, Kenneth Aldape‡, Soonmee Cha‖, and Michael D. Kuo*,**††

7 gene "modules"

with coherent patterns of variations

10 MRI imaging semantic features

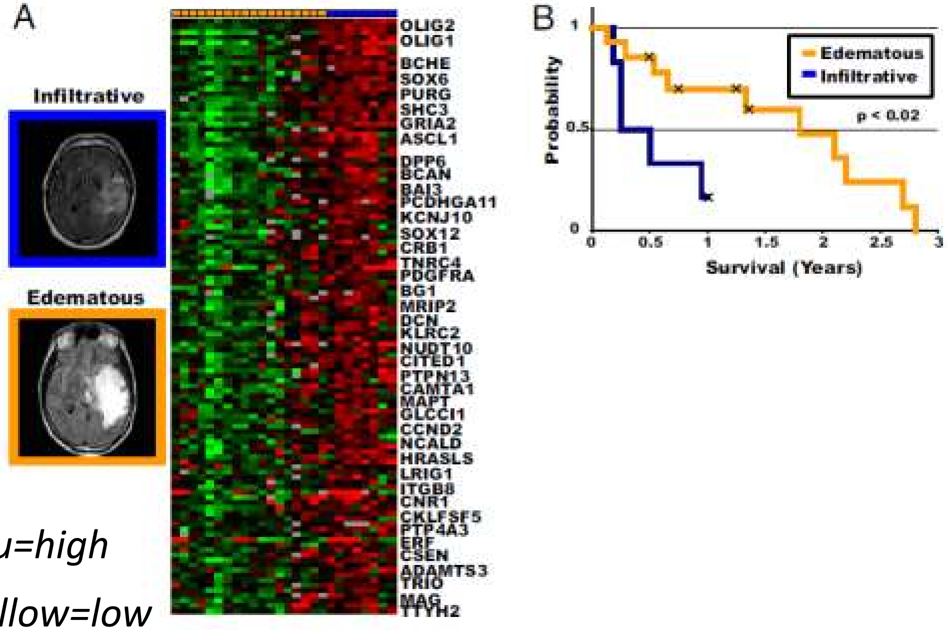

Blu=high

Yellow=low

Image features and genomics

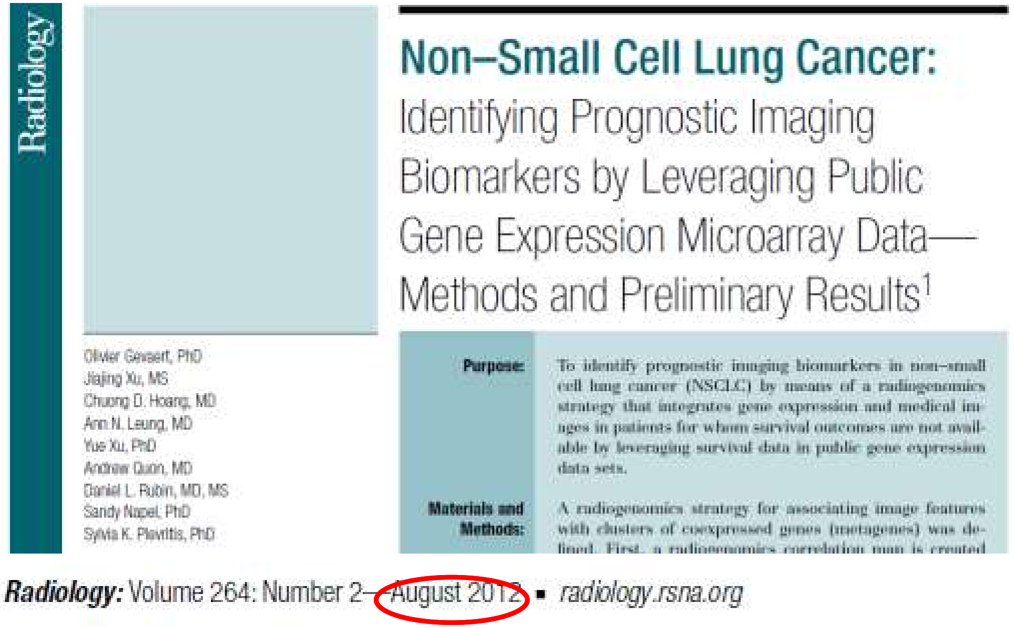

Radiology

Non–Small Cell Lung Cancer: Identifying Prognostic Imaging Biomarkers by Leveraging Public Gene Expression Microarray Data—Methods and Preliminary Results[1]

Olivier Gevaert, PhD
Jiajing Xu, MS
Chuong D. Hoang, MD
Ann N. Leung, MD
Yue Xu, PhD
Andrew Quon, MD
Daniel L. Rubin, MD, MS
Sandy Napel, PhD
Sylvia K. Plevritis, PhD

Purpose: To identify prognostic imaging biomarkers in non–small cell lung cancer (NSCLC) by means of a radiogenomics strategy that integrates gene expression and medical images in patients for whom survival outcomes are not available by leveraging survival data in public gene expression data sets.

Materials and Methods: A radiogenomics strategy for associating image features with clusters of coexpressed genes (metagenes) was defined. First, a radiogenomics correlation map is created

Radiology: Volume 264: Number 2—August 2012 ▪ radiology.rsna.org

Non-Small Cell lung cancer

4 CT image features correlated with metagenes

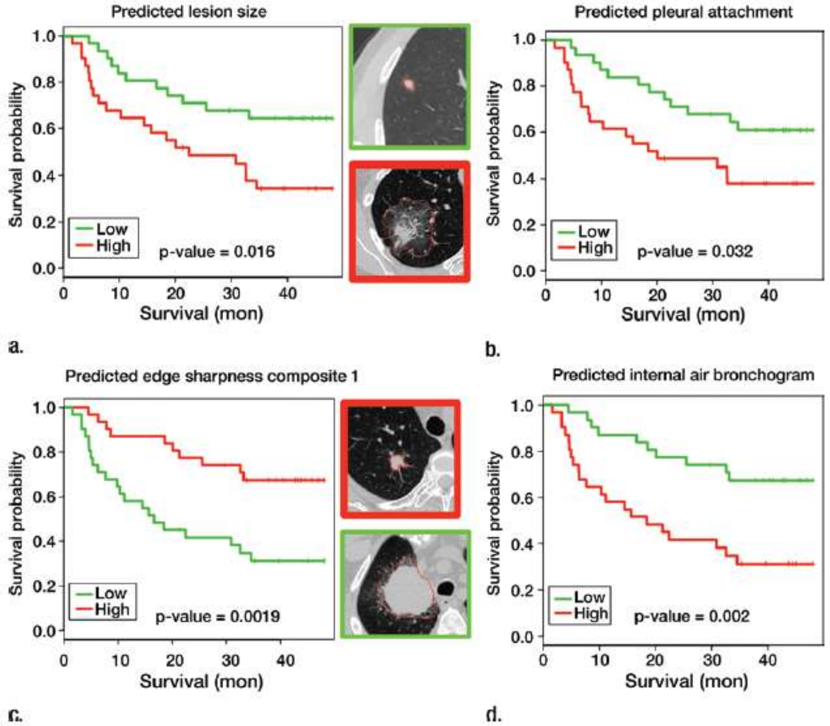

153 CT features

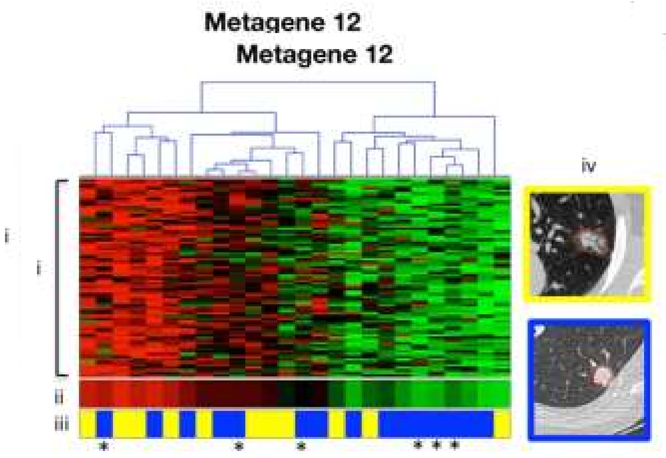

Statistical image features computation example for RadiOmics

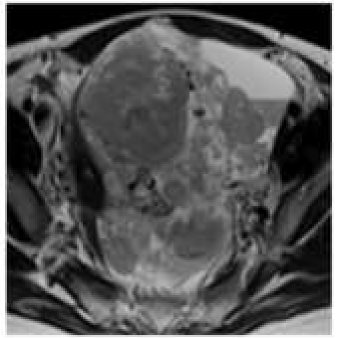

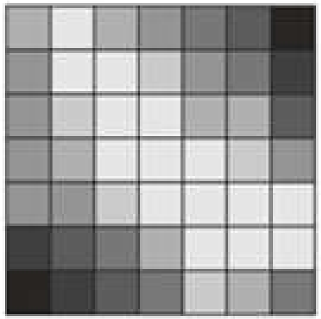

Image intensity values

3	1	3	4	5	6	8
4	1	1	2	4	5	7
4	2	1	1	3	3	6
4	3	1	1	1	2	4
4	4	2	1	1	1	1
7	6	5	3	1	1	1
8	7	6	5	2	3	5

Map of frequency of intensity values

Map of probability of frequencies

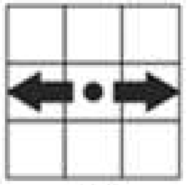

0°

	1	2	3	4	5	6	7	8
1	18	4	5	1	0	0	0	0
2	4	0	1	4	1	0	0	0
3	5	1	2	2	2	1	0	0
4	1	4	2	2	2	0	0	0
5	0	1	2	2	0	3	1	0
6	0	0	1	0	3	0	2	1
7	0	0	0	0	1	2	0	1
8	0	0	0	0	0	1	1	0

$\Sigma=84$

	1	2	3	4	5	6	7	8
1	0.21	0.05	0.06	0.01	0.00	0.00	0.00	0.00
2	0.05	0.00	0.01	0.05	0.01	0.00	0.00	0.00
3	0.06	0.01	0.02	0.02	0.02	0.01	0.00	0.00
4	0.01	0.05	0.02	0.02	0.02	0.00	0.00	0.00
5	0.00	0.01	0.02	0.02	0.00	0.04	0.01	0.00
6	0.00	0.00	0.01	0.00	0.04	0.00	0.02	0.01
7	0.00	0.00	0.00	0.00	0.01	0.02	0.00	0.01
8	0.00	0.00	0.00	0.00	0.00	0.01	0.01	0.00

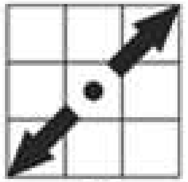

45°

	1	2	3	4	5	6	7	8
1	8	5	6	6	2	0	0	0
2	5	0	0	1	1	2	0	0
3	6	0	0	1	1	1	1	0
4	6	1	1	0	0	1	1	0
5	2	1	1	0	0	0	1	1
6	0	2	1	1	0	0	0	1
7	0	0	1	1	1	0	0	0
8	0	0	0	0	1	1	0	0

$\Sigma=72$

	1	2	3	4	5	6	7	8
1	0.11	0.07	0.08	0.08	0.03	0.00	0.00	0.00
2	0.07	0.00	0.00	0.01	0.01	0.03	0.00	0.00
3	0.08	0.00	0.00	0.01	0.01	0.01	0.01	0.00
4	0.08	0.01	0.01	0.00	0.00	0.01	0.01	0.00
5	0.03	0.01	0.01	0.00	0.00	0.00	0.01	0.01
6	0.00	0.03	0.01	0.01	0.00	0.00	0.00	0.01
7	0.00	0.00	0.01	0.01	0.01	0.00	0.00	0.00
8	0.00	0.00	0.00	0.00	0.01	0.01	0.00	0.00

3x3

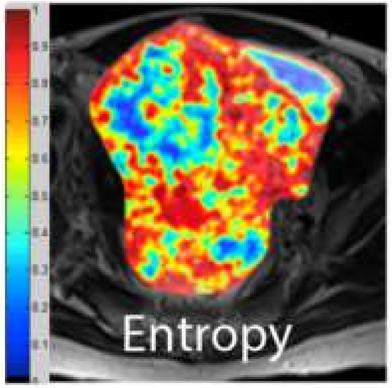

Total Entropy = 1,43

Radiomics: a new approach for the study of cancer

HHS Public Access
Author manuscript
Eur J Cancer. Author manuscript; available in PMC 2015 August 12.

Published in final edited form as:
Eur J Cancer. 2012 March ; 48(4): 441–446. doi:10.1016/j.ejca.2011.11.036.

Radiomics: Extracting more information from medical images using advanced feature analysis

Philippe Lambin[a,*,e,f], Emmanuel Rios-Velazquez[a,e], Ralph Leijenaar[a,e], Sara Carvalho[a,e], Ruud G.P.M. van Stiphout[a,e], Patrick Granton[a,e], Catharina M.L. Zegers[a,e], Robert Gillies[b,e], Ronald Boellard[c,e], André Dekker[a,e], and Hugo J.W.L. Aerts[a,d,e]

[a]Department of Radiation Oncology (MAASTRO), GROW – School for Oncology and Developmental Biology, Maastricht University Medical Center, Maastricht, The Netherlands [b]H. Lee Moffitt Cancer Center and Research Institute, Tampa, FL, USA [c]U University Medical Center, Department of Nuclear Medicine & PET Research, Amsterdam, The Netherlands [d]Computational Biology and Functional Genomics Laboratory, Department of Biostatistics and Computational Biology, Dana-Farber Cancer Institute, Harvard School of Public Health, USA

Comprehensive quantification of disease phenotypes by applying <u>a large number of quantitative image features</u> representing lesion heterogeneity and correlating with omics and clinical data

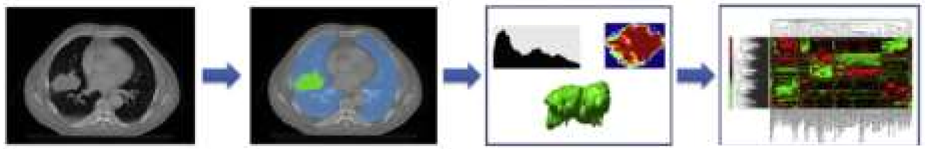

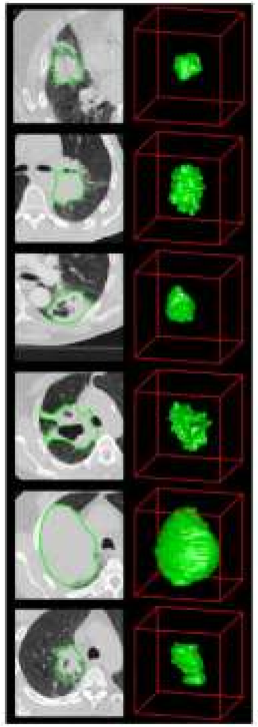

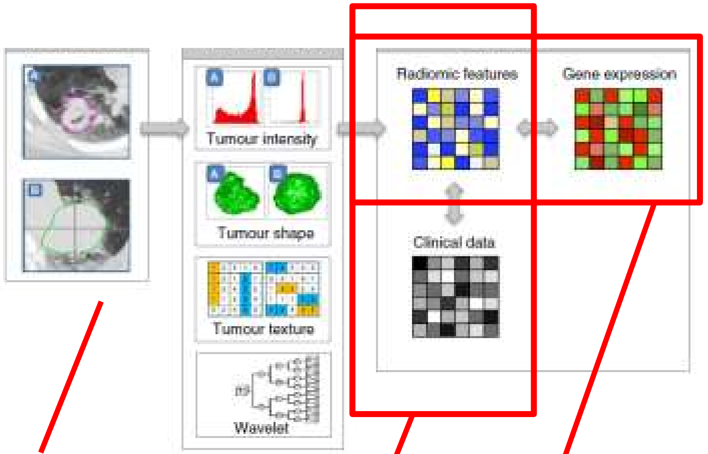

Partition - Segmentation) of image (biobank)

RadiOmics

RadiogenOmics

<u>Morphological and architectural Quantitative features</u>

Predictive models based on radiomic signatures


www.nature.com/scientificreports

SCIENTIFIC REPORTS

OPEN

Machine Learning methods for Quantitative Radiomic Biomarkers

Radiomics extracts and mines large number of medical imaging features quantifying tumor phenotypic characteristics. Highly accurate and reliable machine-learning approaches can drive the

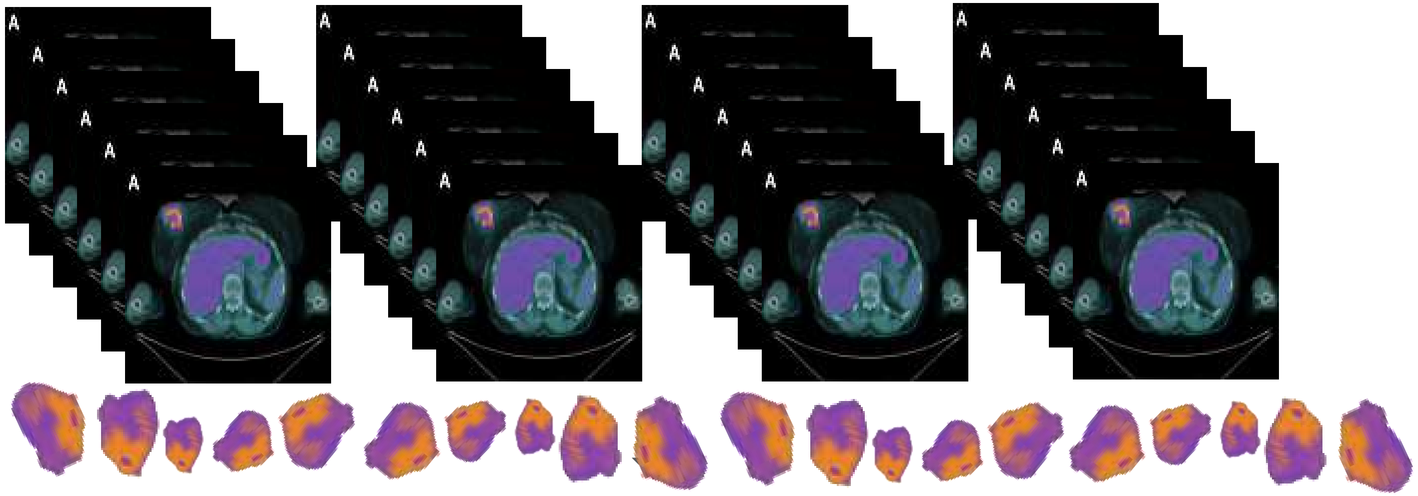

Partitions of image (biobanks)

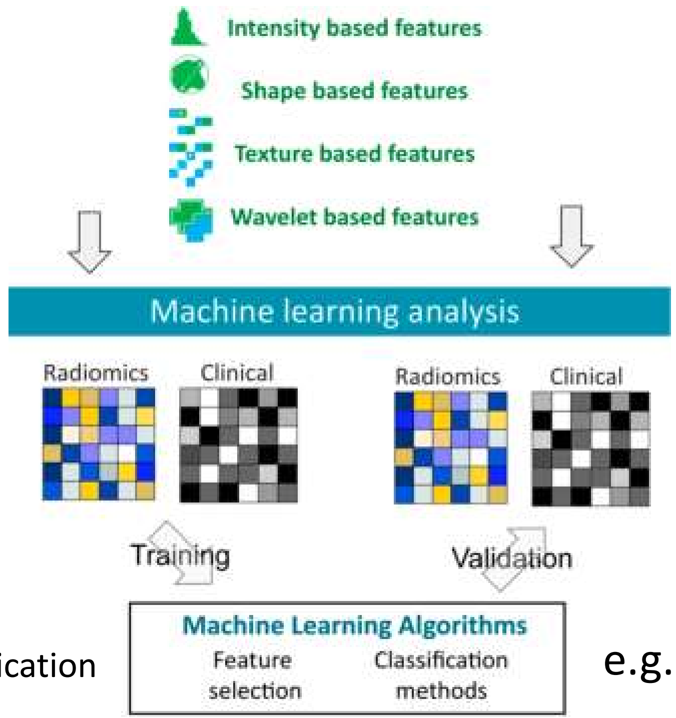

To automatically predict clinical outcome at the level of single patient by training and validating machine learning models with radiOmics features

*St Gallen classification

e.g.. Accuracy >0.85

PET radiomic predicts breast cancer subtypes

**patients with breast cancer prior biopsy*

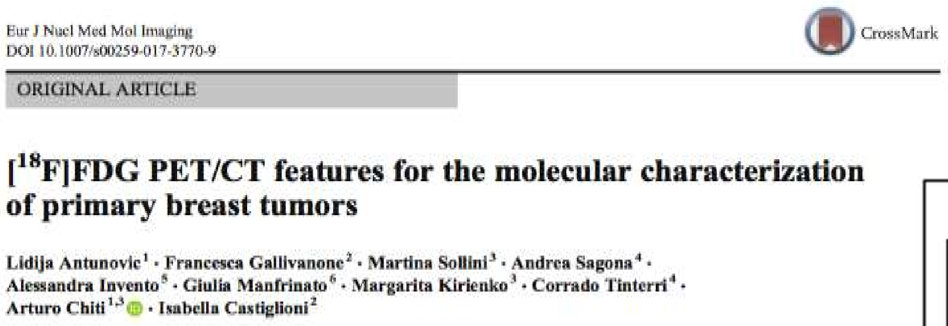
Eur J Nucl Med Mol Imaging
DOI 10.1007/s00259-017-3770-9
CrossMark

ORIGINAL ARTICLE

[^{18}F]FDG PET/CT features for the molecular characterization of primary breast tumors

Lidija Antunovic[1] · Francesca Gallivanone[2] · Martina Sollini[3] · Andrea Sagona[4] · Alessandra Invento[5] · Giulia Manfrinato[6] · Margarita Kirienko[3] · Corrado Tinterri[4] · Arturo Chiti[1,3] · Isabella Castiglioni[2]

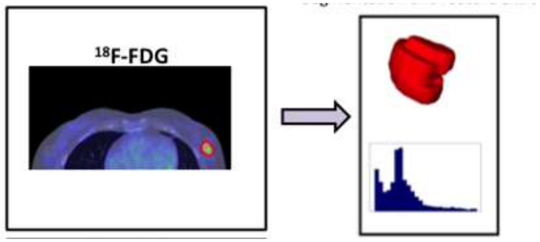

PET features

PVC-SUV$_{mean}$
PVC- TLG
Median
Energy
Entropy
Kurtosis
Skewness
Uniformity
Variance
Surface Area
Sphericity
Surface to Volume ratio
....

PET radiomic features vs himmunochemistry molecular factors and molecular subtypes (5)*

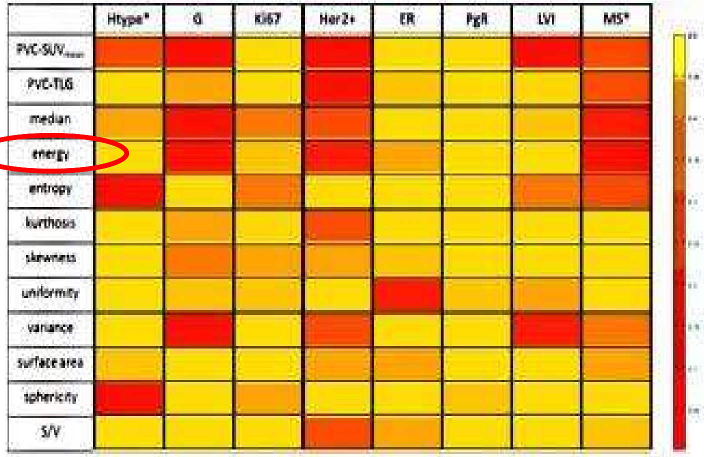

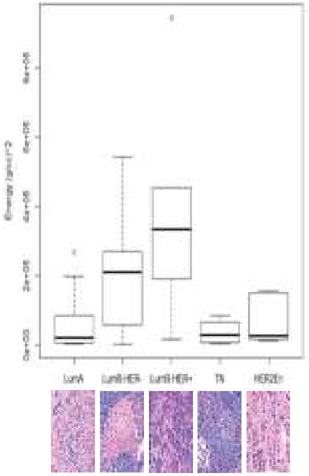

*St Gallen classification

MRI-DWI radiomic predicts breast cancer treatment response

Magn Reson Mater Phy (2017) 30:359–373
DOI 10.1007/s10334-017-0610-7

RESEARCH ARTICLE

Biomarkers from in vivo molecular imaging of breast cancer: pretreatment ^{18}F-FDG PET predicts patient prognosis, and pretreatment DWI-MR predicts response to neoadjuvant chemotherapy

Francesca Gallivanone[1] · Marta Maria Panzeri[2] · Carla Canevari[3] · Claudio Losio[2] · Luigi Gianolli[3] · Francesco De Cobelli[2,4] · Isabella Castiglioni[1]

**38 Breast cancer patients treated with NAC + surgery*

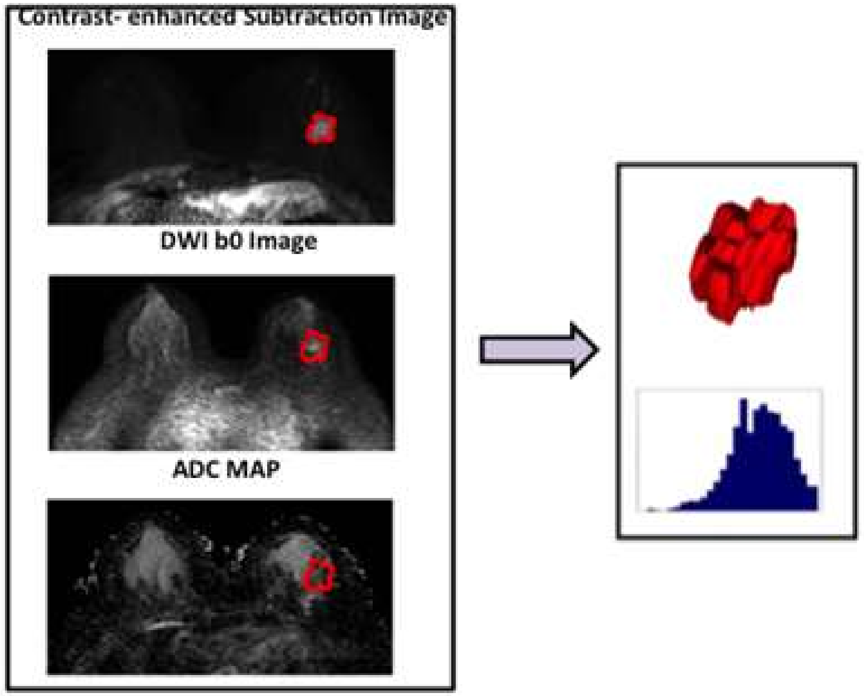

MRI-DWI radiomic features VS NAC pCR

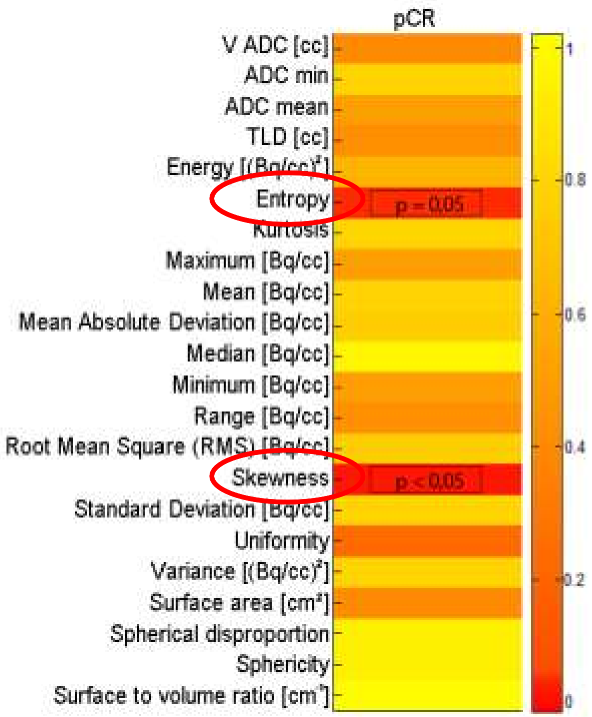

PET radiomic predicts lung cancer treatment

[Frontiers In Bioscience, Landmark, 22, 1713-1723, June 1, 2017]

FDG PET/CT as theranostic imaging in diagnosis of non-small cell lung cancer

Margarita Kirienko[1], Francesca Gallivanone[2], Martina Sollini[1], Giulia Veronesi[3], Emanuele Voulaz[3], Lidjia Antunovic[4], Lorenzo Leonardi[4], Giorgio Testanera[4], Isabella Castiglioni[2], Arturo Chiti[1,4]

[1]Department of Biomedical Sciences, Humanitas University, Rozzano, Milan, Italy, [2]IBFM-CNR, Segrate, Milan, Italy, [3]Thoracic Surgery, Humanitas Clinical and Research Center, Rozzano, Milan, Italy, [4]Nuclear Medicine, Humanitas Clinical and Research Center, Rozzano, Milan, Italy

**Non-Small Cell lung cancer patients treated with surgery + NAC*

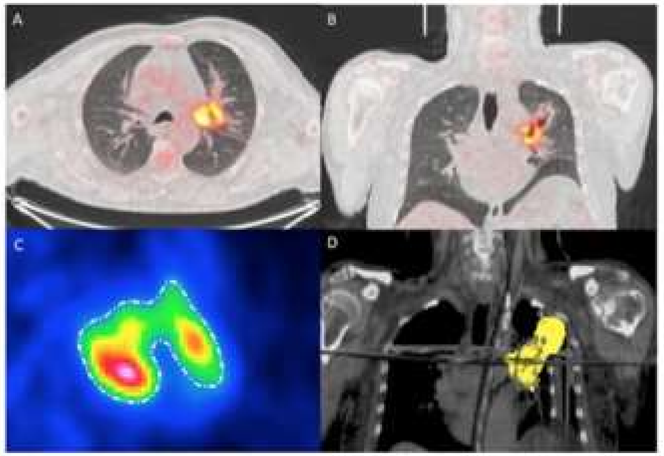

Figure 1. A 67-year-old male with squamous cell carcinoma, G3pT3N1 (stage IIIa) who underwent pneumonectomy and subsequent adjuvant chemotherapy with cisplatin and vinorelbine. After 36 months' follow-up the patient had no evidence of disease. PVC-SUV = 15.59 g/cc, SUVmax = 21.18 g/cc, Energy = 3.2E08 (g/cc)2, Entropy = 4.08, Kurtosis = 3.85. The axial (A) and coronal (B) fused PET/CT images show the lesion in the upper left lobe; the axial PET (C) image shows the tumour segmentation operated by the algorithm; (D) metabolic tumour volume visualized on CT images.

Survival endpoint	PET feature	P-value	Cut-off	Sensitivity	Specificity
DSF	Energy[(MBq/cc)²]	0.01	2.74	87.5%	75%
	Kurtosis	<0.05	2.71	75%	60%
DMFS	PVC-SUV_{mean}	<0.05	11.91	80%	80%
	SUV_{max}	<0.05	14.84	80%	80%
	Energy[(MBq/cc)²]	<0.05	2.74	100%	80%
	Kurtosis	<0.05	2.9	100%	75%

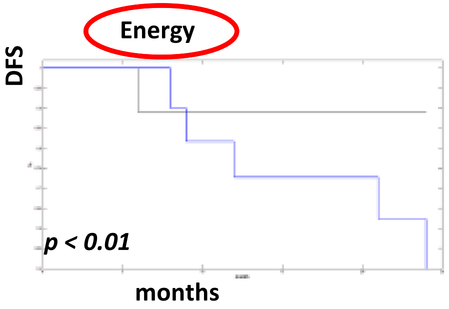

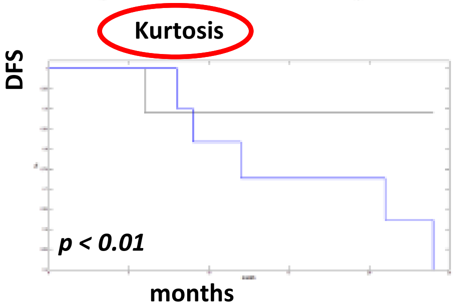

Decision support systems in clinical medicine

- decision support systems, designed to increase the effectiveness of the medical analysis as it provides support to clinicians who need to make strategic medical decisions in the face of a medical problems that can not be solved with operational research models

- extract from a significant amount of data, in a short time and in a versatile way, new information useful to the clinical decision-making processes

- Assisted Diagnosis
- Objective clinical assessment
- High diagnostic accuracy

In vivo imaging plays a new role in the diagnostic process of many diseases

[e.g. McKhann GM et al. The diagnosis of dementia due to Alzheimer's disease: Recommendations from the National Institute on Aging-Alzheimer's Association workgroups on diagnostic guidelines for Alzheimer's disease. Alzheimer's & Dementia 7(3): 263-69. (2011)]

Decision support systems in clinical medicine

publications per year from 1965 to 2015

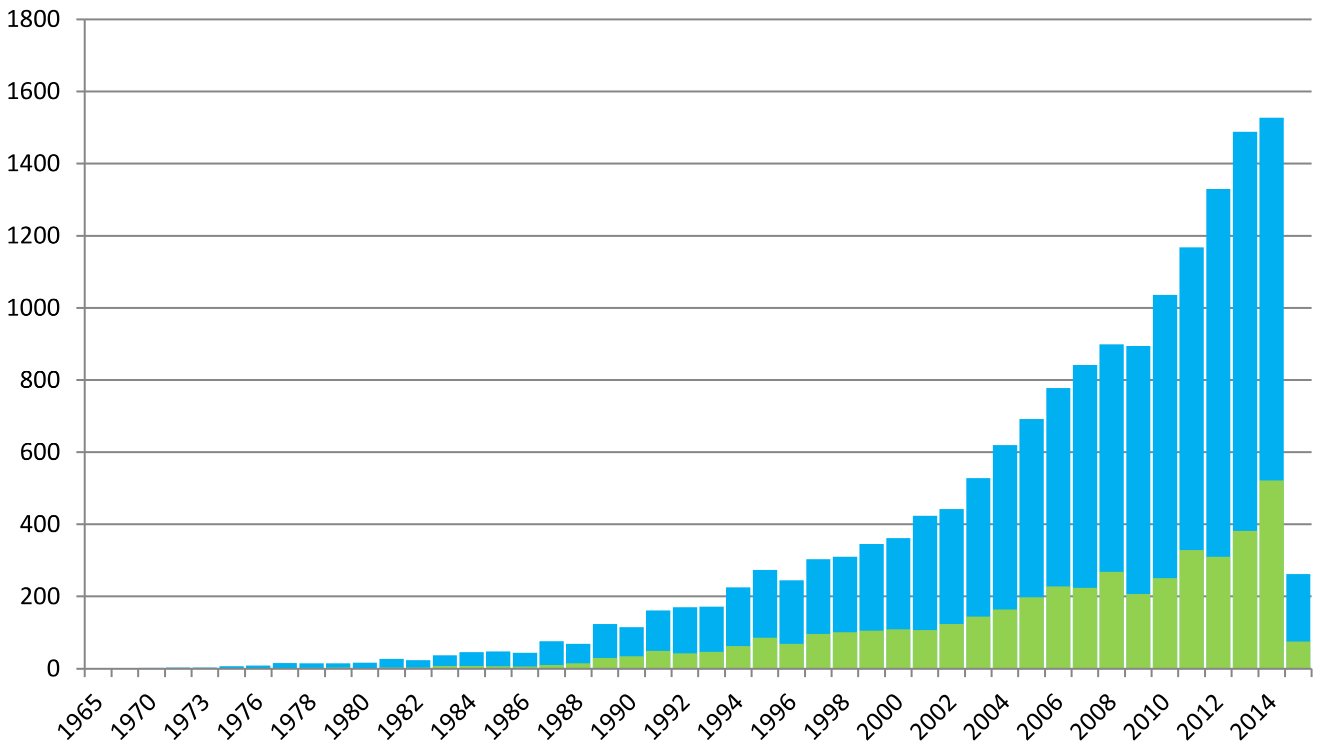

RESEARCH CRITERIA:

"decision support system"

"decision support system medicine"

source: pubmed.com

Machine learning applied to medical imaging

. how is this useful in medicine?

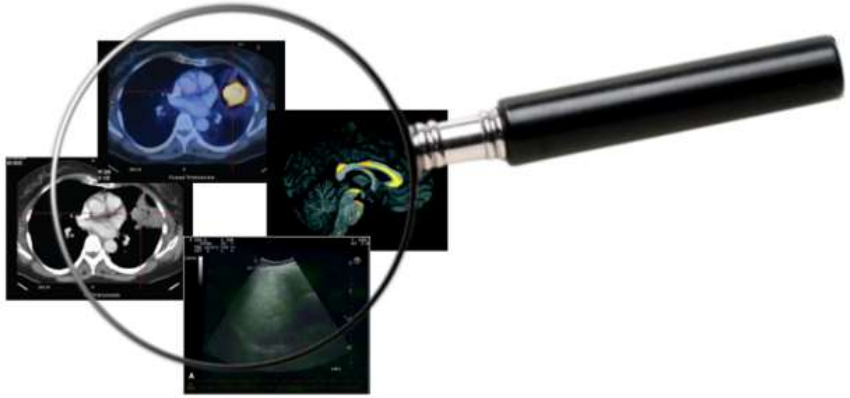

Reference standard for the AI model

- Reference Standard
- Gold Standard
- Ground truth

It defines the clinical condition to be predicted
(i.e. diagnostic subtype, prognostic subtype, treatment response subtype)!

Reference standard for the training of the AI model

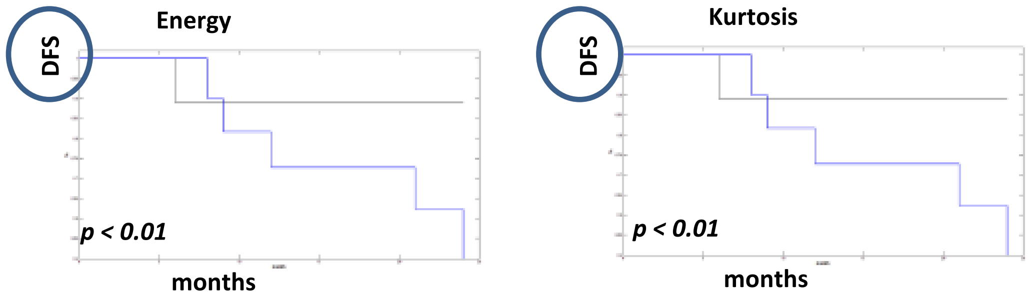

- *Clinical follow-up endpoint (disease-free-survival DFS, overall survival OS, …)*
- *Histological diagnosis from biopsy*
- *Histological diagnosis from biopsy and definite surgery*
- *Molecular diagnosis*
- *Radiological classification*
- *Treatment response*

….

Machine learning applied to medical imaging

Machine learning applied to medical imaging

Machine learning applied to medical imaging

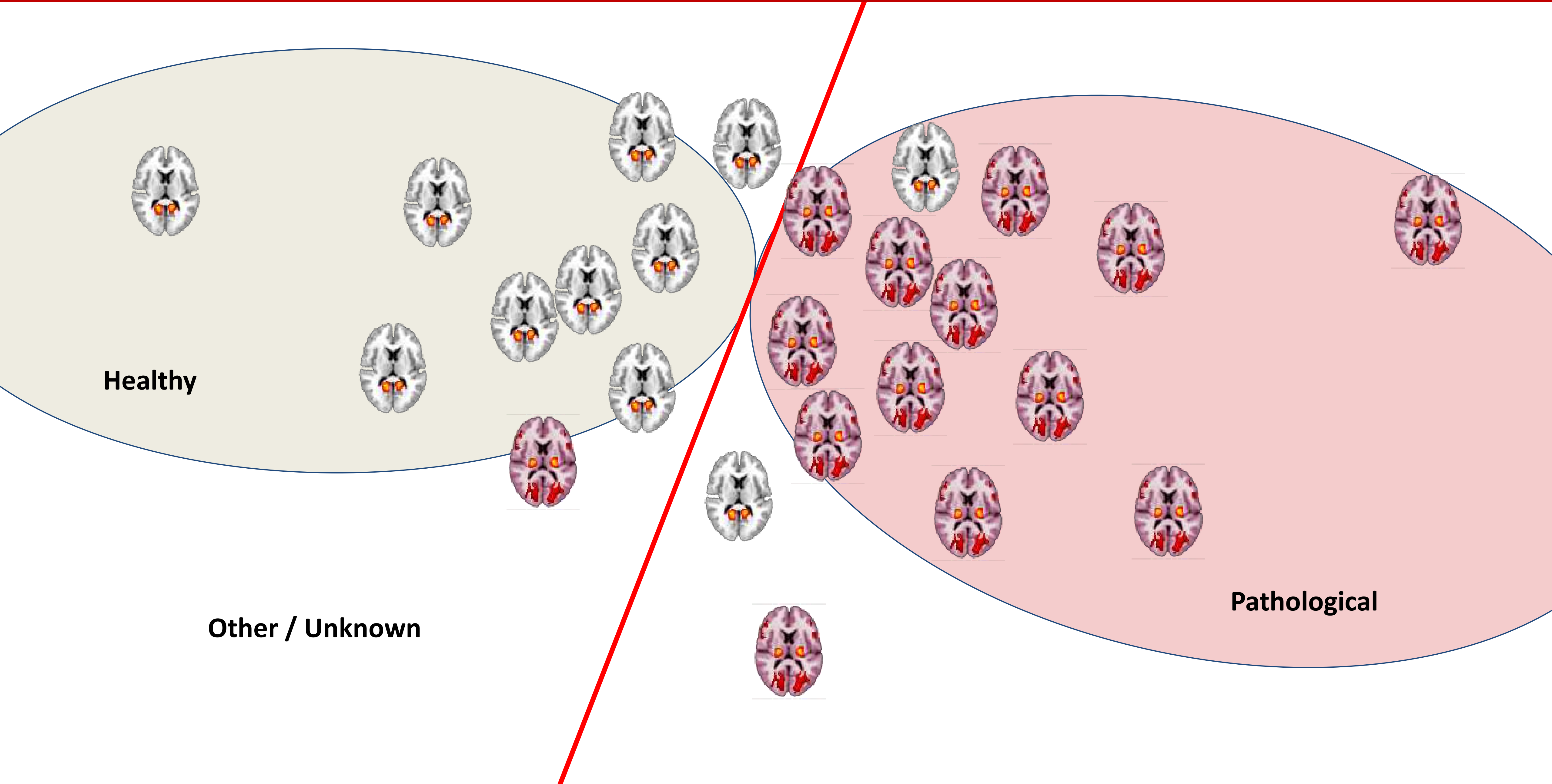

Machine learning applied to medical imaging

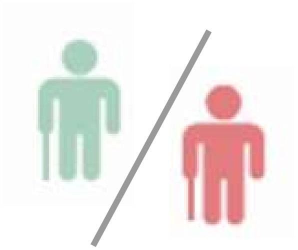

Diagnosis (early/differential)

is the patient healthy?

Prognosis

what will be the course of the disease?

Screening

are the patients -within a population- healthy?

Treatment addressing

will this therapy be effective for this patient?

ML Models | Examples
(using different types of data)

ML models | Examples

Alzheimer's Disease

ML models | Examples

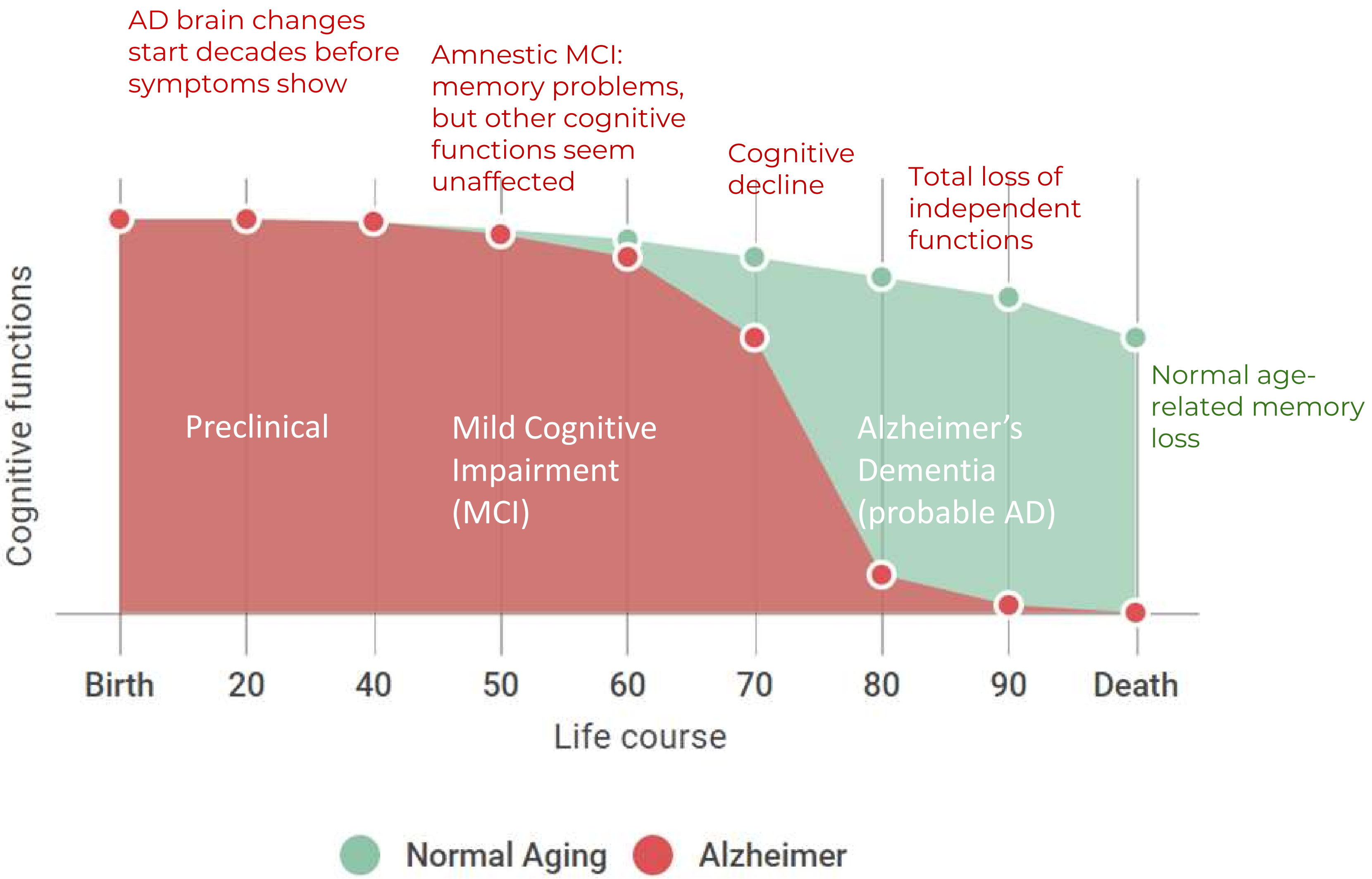

ML models | Examples

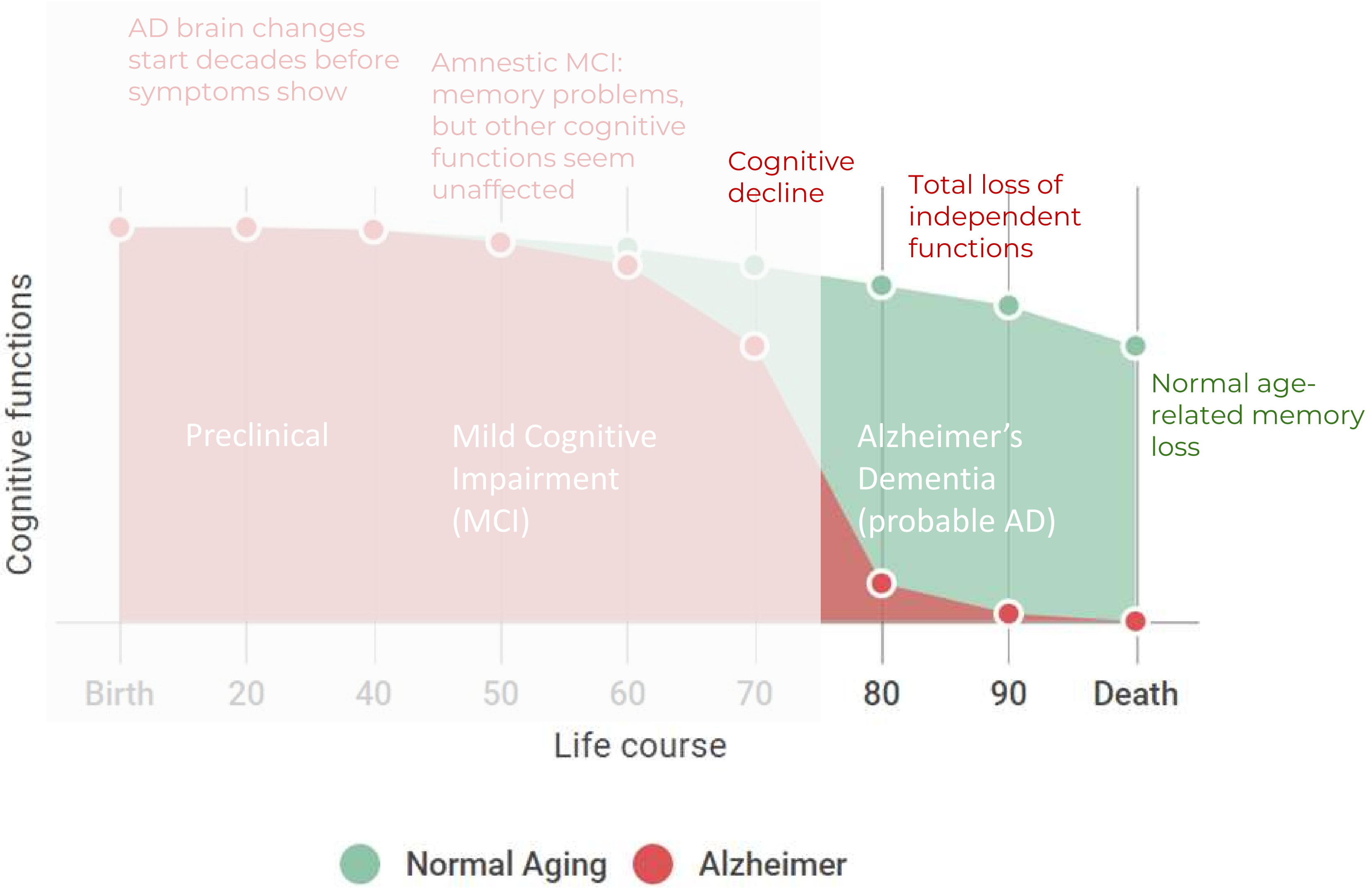

ML models | Examples

Clinical Diagnosis of Alzheimer’s Disease

162	134	76	137
CN	MCInc	MCIc	AD

A dataset
of 509 subjects

Structural MRI
T1 weighted
1.5 Tesla

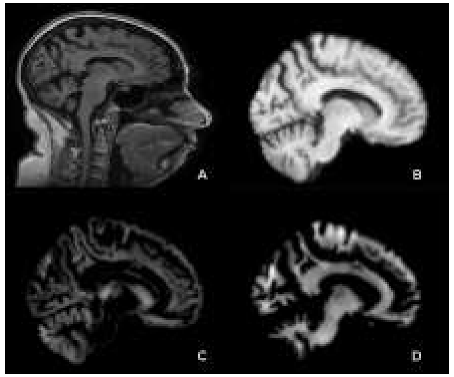

AD **Alzheimer’s Disease**
MCIc Mild Cognitive Impairment, converting to Alzheimer’s Dementia
MCInc Mild Cognitive Impairment, not converting to Alzheimer’s Dementia
CN Cognitively-Normal subjects

Magnetic resonance imaging biomarkers for the early diagnosis of Alzheimer's disease: A machine learning approach.
Salvatore et al. 2015, Frontiers in Neuroscience.

ML models | Examples

Clinical Diagnosis			Accuracy (automatic classification)
AD	vs	CN	76%
MCIc	vs	CN	72%
MCIc	vs	MCInc	66%

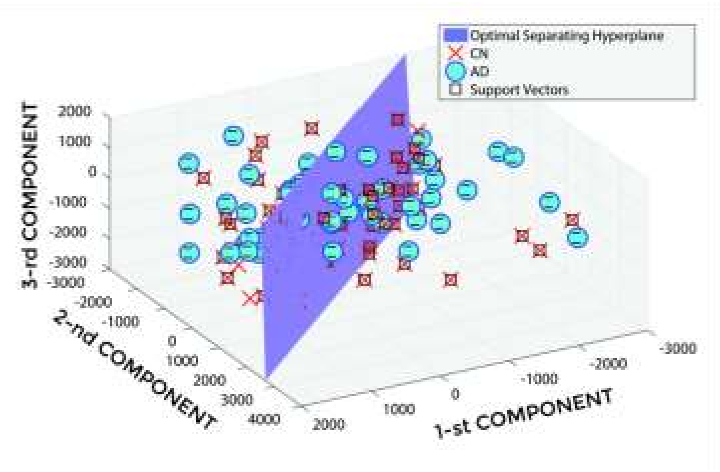

Magnetic resonance imaging biomarkers for the early diagnosis of Alzheimer's disease: A machine learning approach.
Salvatore et al. 2015, Frontiers in Neuroscience.

ML models | Examples

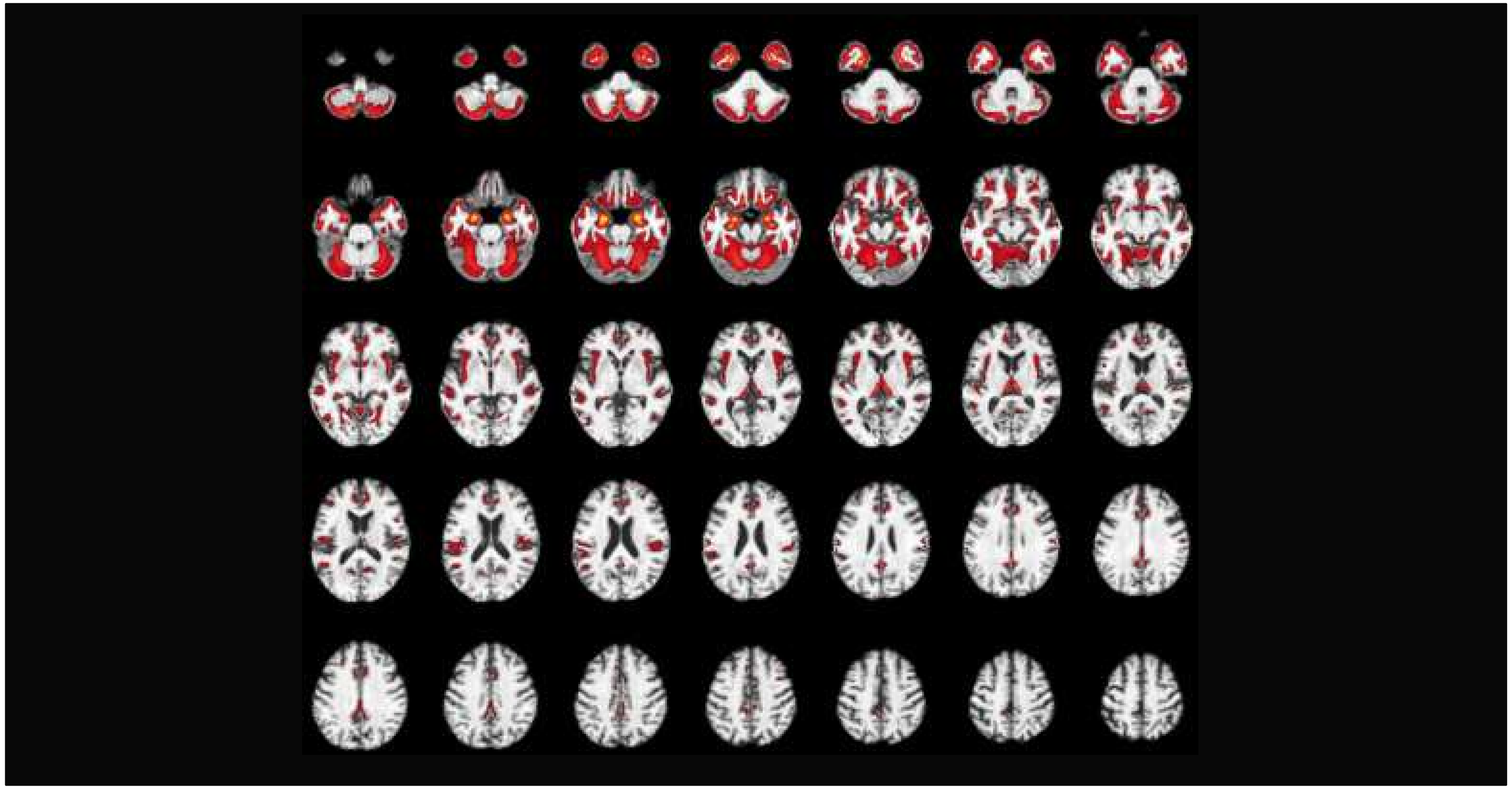

Best Structural-MRI Predictors

AD vs CN

Magnetic resonance imaging biomarkers for the early diagnosis of Alzheimer's disease: A machine learning approach.
Salvatore et al. 2015, Frontiers in Neuroscience.

ML models | Examples

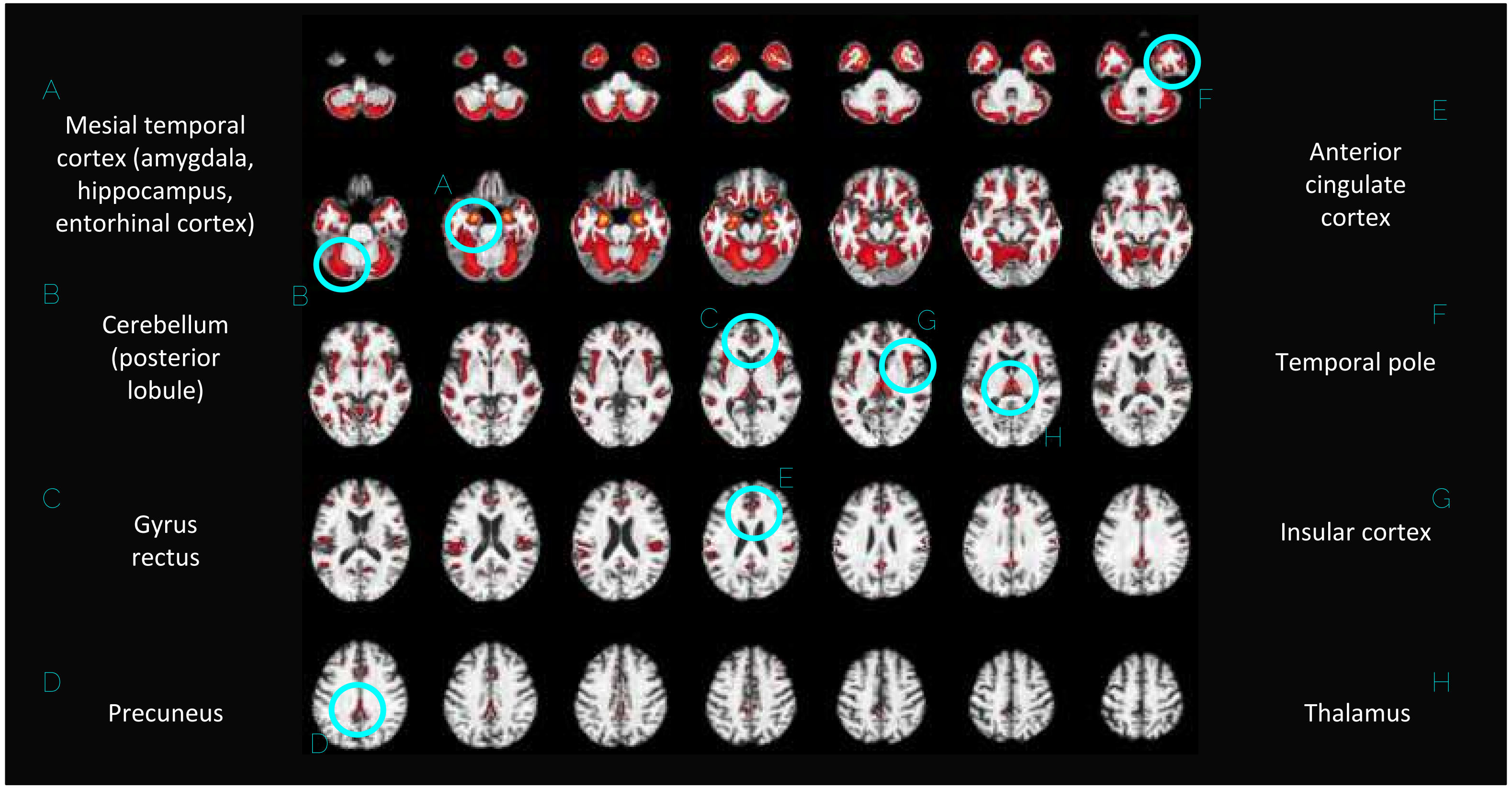

Best Structural-MRI Predictors

AD vs CN

Magnetic resonance imaging biomarkers for the early diagnosis of Alzheimer's disease: A machine learning approach.
Salvatore et al. 2015, Frontiers in Neuroscience.

ML models | Examples

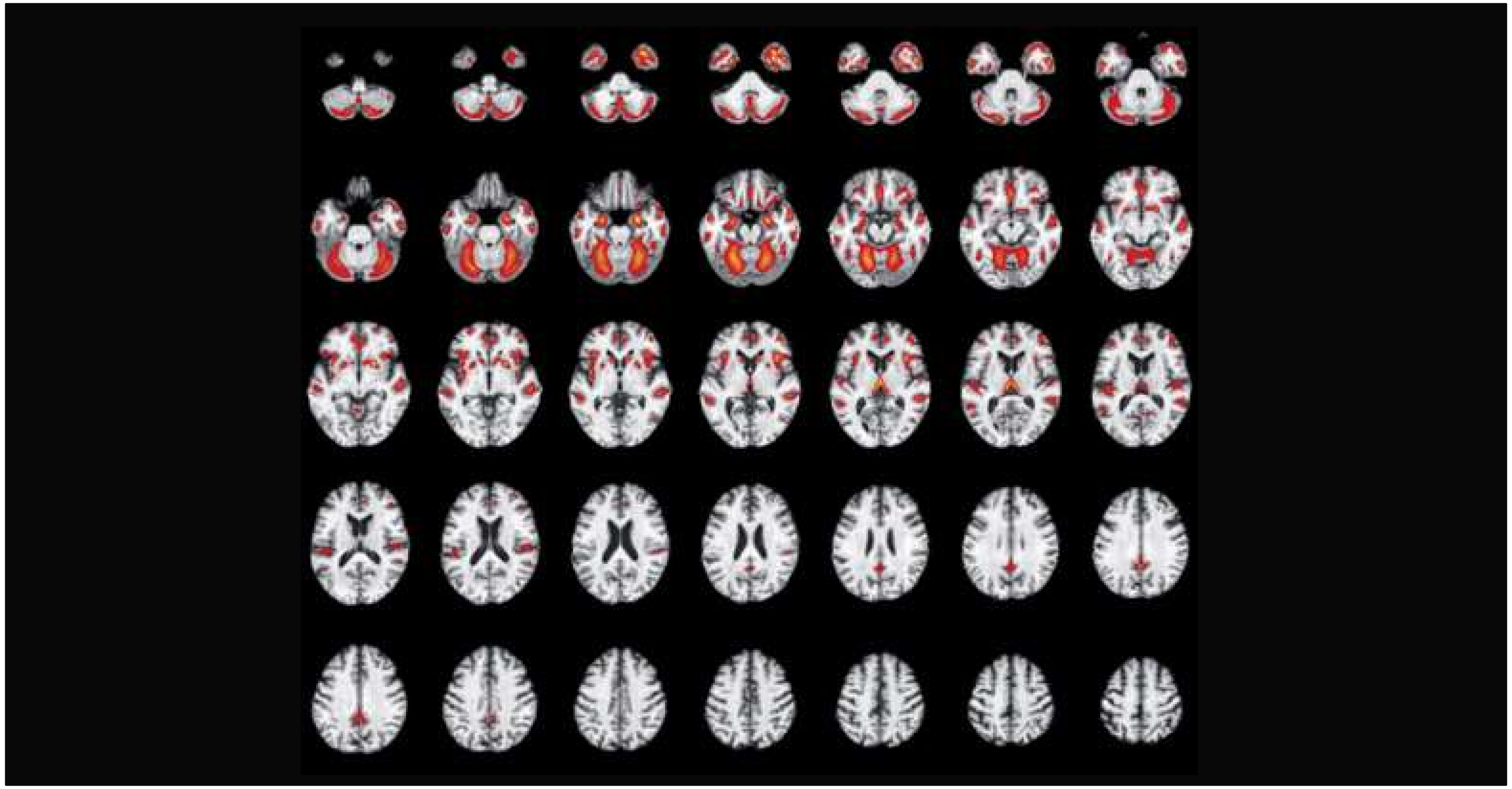

Best Structural-MRI Predictors

MCIc vs CN

Magnetic resonance imaging biomarkers for the early diagnosis of Alzheimer's disease: A machine learning approach.
Salvatore et al. 2015, Frontiers in Neuroscience.

ML models | Examples

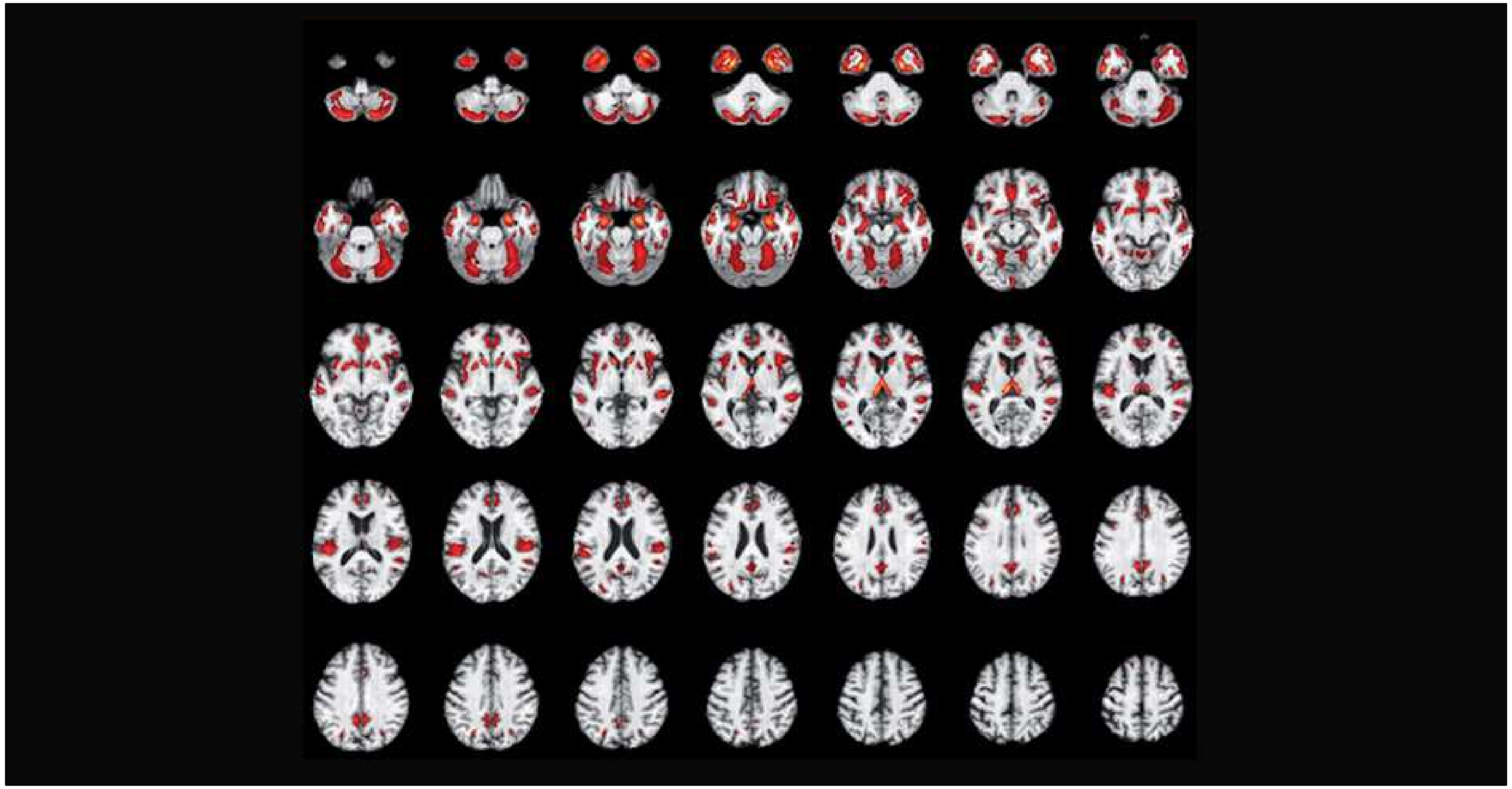

Best Structural-MRI Predictors

MCIc vs MCInc

Magnetic resonance imaging biomarkers for the early diagnosis of Alzheimer's disease: A machine learning approach.
Salvatore et al. 2015, Frontiers in Neuroscience.

ML models | Examples

Clinical Diagnosis of AD at 24 months follow up

50 50 50 50

CN MCInc MCIc AD

A dataset
of 200 subjects

Structural MRI
T1 weighted
1.5 Tesla

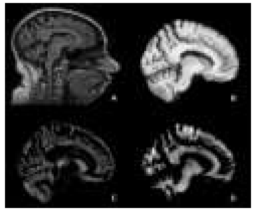

65 scores/subscores
from 7 neuro-
psychological tests

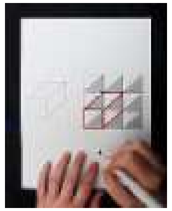

Measure #1 | Measure #2 | Measure #3 | Diagnosis

Timeline
months

0 6 12 24

MRI characterizes the progressive course of AD and predicts conversion to Alzheimer's dementia twenty-four months before probable diagnosis. *Salvatore et al. 2018, Frontiers in Aging Neuroscience.*

ML models | Examples

Clinical Diagnosis (24 months follow up)

AD + MCIc

vs

MCInc + CN

Accuracy (sen/spe)

79% (79/78)	85% (83/87)
MRI	**MRI + NPS**

24 months before stable diagnosis

MRI characterizes the progressive course of AD and predicts conversion to Alzheimer's dementia twenty-four months before probable diagnosis. *Salvatore et al. 2018, Frontiers in Aging Neuroscience.*

ML models | Examples

Best Neuropsychological Predictors

24 months before stable diagnosis

Ability in remembering appointments, family occasions, holidays, medications in FAQ
Functional abilities

Ability in writing checks, paying bills, or balancing checkbook in FAQ
Functional abilities

Ability in assembling tax records, business affairs in FAQ
Functional abilities

Total score of trial 5 in AVLT
Memory and learning

Ability in keeping track of current events in FAQ
Functional abilities

Total intrusions of trial 1 in AVLT
Memory and learning

Correct answers in the Backwards task in Digit-Span Test
Working memory

Correct answers in Vegetables task in Category Fluency Test
Language

Correct answers after a 30-min delay in AVLT
Memory and learning

MRI characterizes the progressive course of AD and predicts conversion to Alzheimer's dementia twenty-four months before probable diagnosis. *Salvatore et al. 2018, Frontiers in Aging Neuroscience.*

ML models | Examples

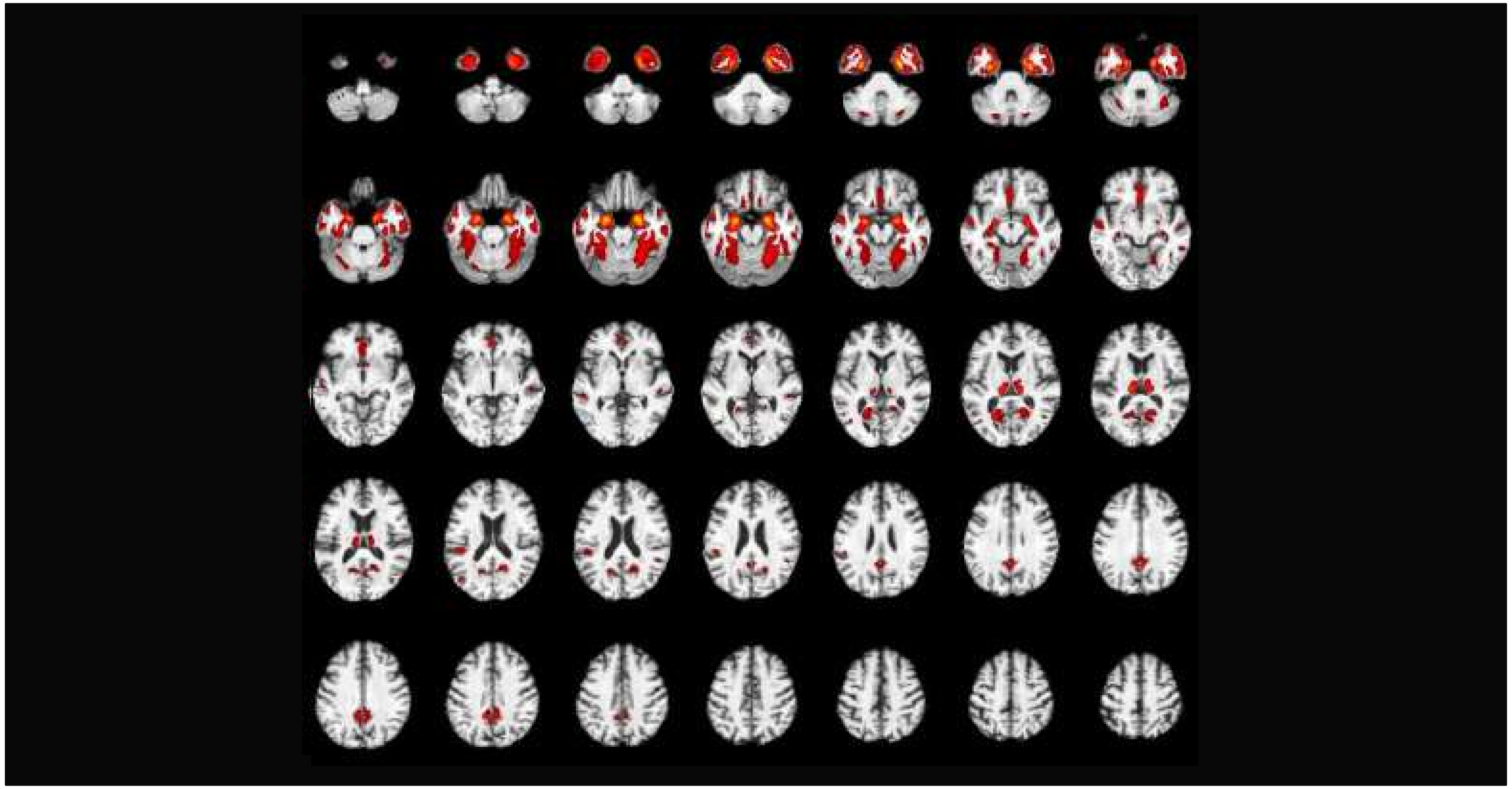

Best Structural-MRI Predictors

24 months before stable diagnosis

MRI characterizes the progressive course of AD and predicts conversion to Alzheimer’s dementia twenty-four months before probable diagnosis. *Salvatore et al. 2018, Frontiers in Aging Neuroscience.*

ML models | Examples

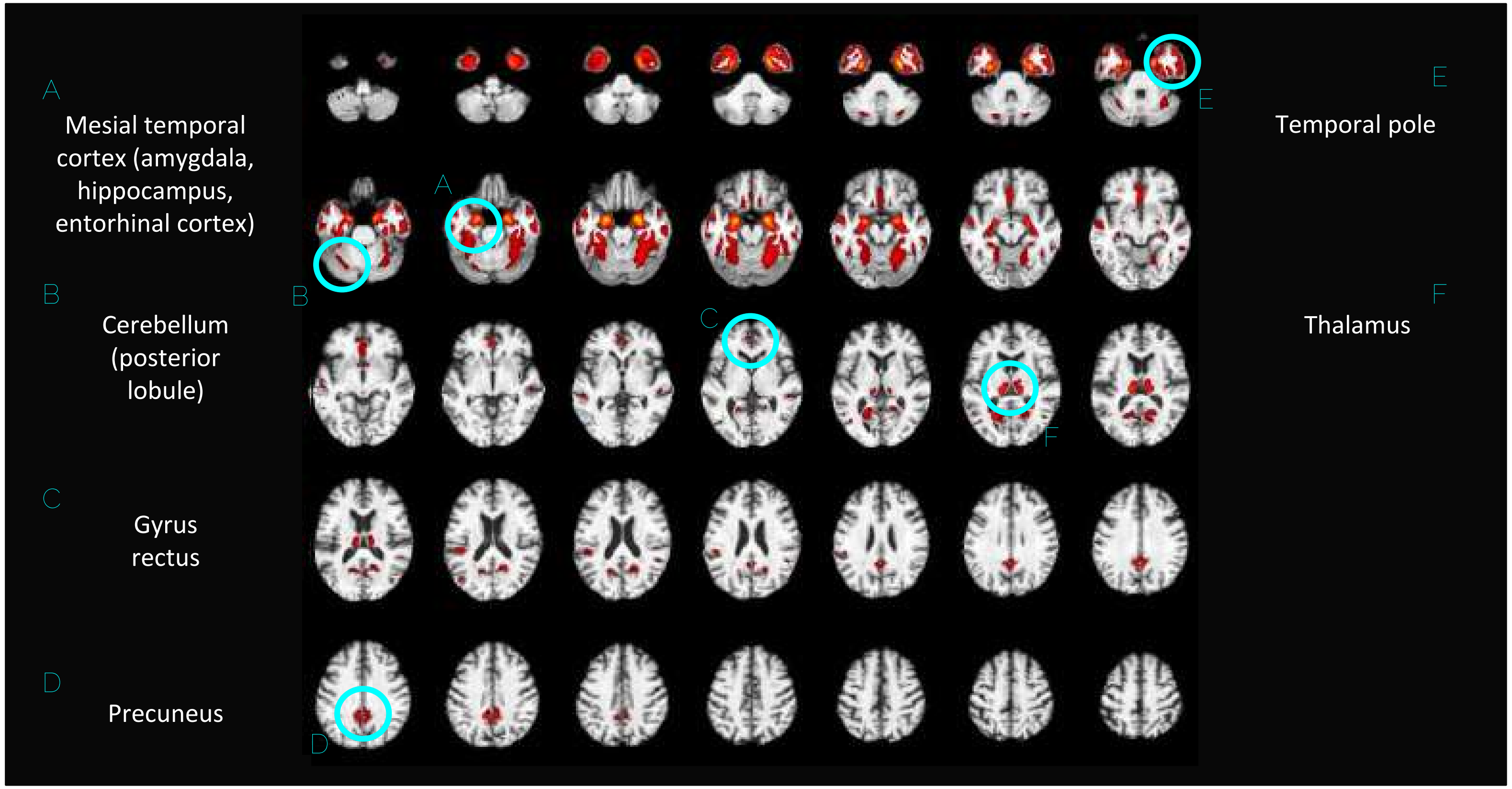

Best Structural-MRI Predictors

24 months before stable diagnosis

MRI characterizes the progressive course of AD and predicts conversion to Alzheimer's dementia twenty-four months before probable diagnosis. *Salvatore et al. 2018, Frontiers in Aging Neuroscience.*

ML models | Examples

Autism Spectrum Disorder

ML models | Examples

Confirm a motor signature of autism

15

TD

15

ASD

A dataset of 30
pre-school children (~3 years old)

17 kinematic features
collected during a reach-to-drop task

ASD **Autism Spectrum Disorder**
TD Typically-developing children

Use of machine learning to identify children with autism and their motor abnormalities. *Crippa, Salvatore et al. 2015, Journal of Autism and Developmental Disorders.*

ML models | Examples

Fig. 1 The experimental task consisted of grasping a rubber ball (**2**) that was placed over a support (see **1**, a); that is, a reach-to-grasp movement before they dropped it in a hole (**3**). The hole (**1**, c) was located inside a see-through *square box* (21 cm high, 20 cm wide) and was large enough not to require fine movements. The goal area is transparent to allow seeing through. 4 markers are placed on the basket under the goal area, 2 on the ball and 3 on each hand (attached to the ulnar and radial surfaces of the participant's wrist and to the hand dorsum on the 4th and 5th metacarpals)

sub-movement 1
the movement necessary to reach the ball and place it on its support

- # movement units
- total movement duration
- peak velocity
- peak acceleration
- time of peak acceleration
- peak deceleration
- time of peak deceleration

sub-movement 2
the movement to transport the ball from a support to the target hole

- # movement units
- total movement duration
- peak velocity
- peak acceleration
- time of peak acceleration
- peak deceleration
- time of peak deceleration
- wrist angle

Use of machine learning to identify children with autism and their motor abnormalities. *Crippa, Salvatore et al. 2015, Journal of Autism and Developmental Disorders.*

ML models | Examples

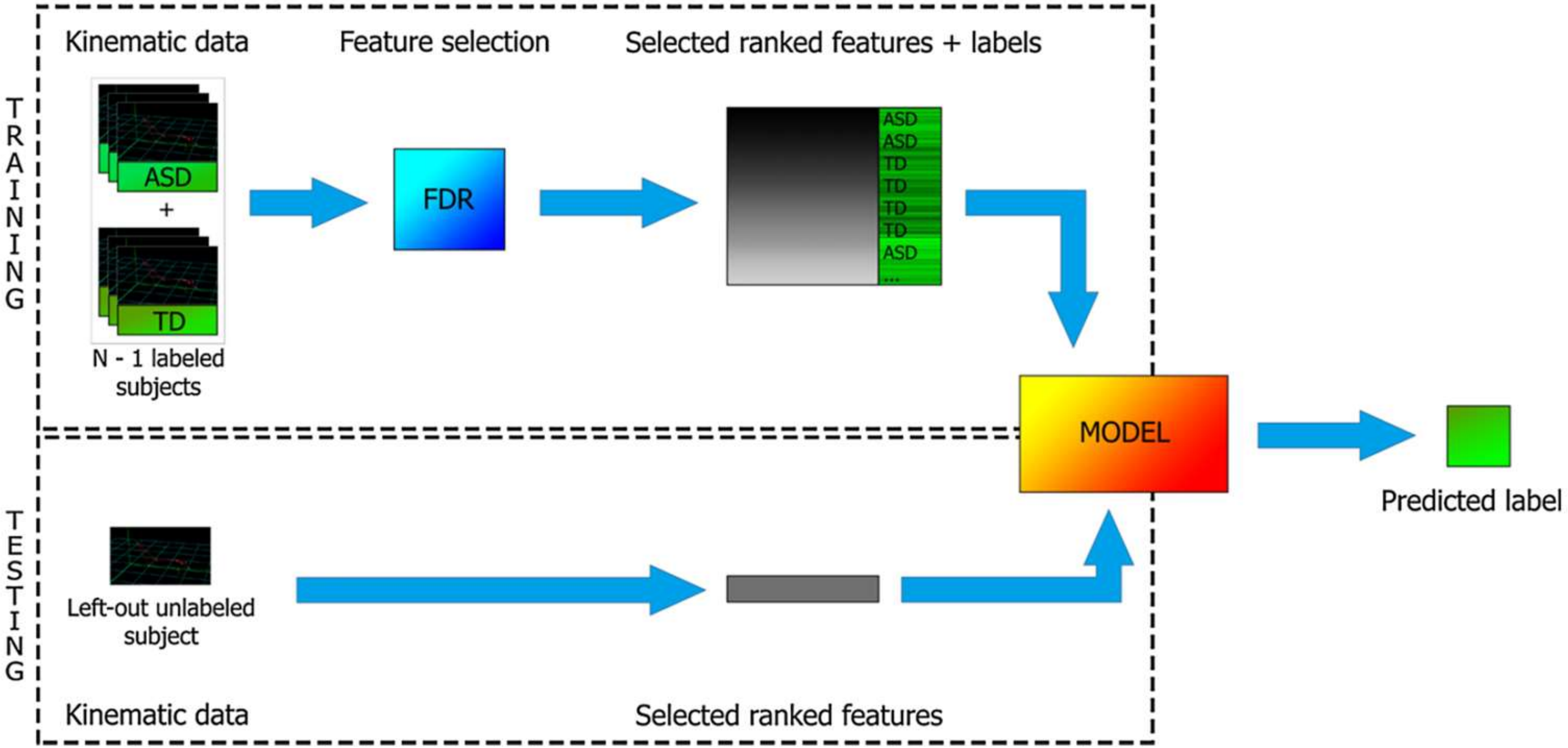

Use of machine learning to identify children with autism and their motor abnormalities. *Crippa, Salvatore et al. 2015, Journal of Autism and Developmental Disorders.*

ML models | Examples

	Overall mean	Optimal configuration
Diagnostic accuracy (sensitivity / specificity)	85 (82/ 89)%	97 (100/ 94)%

Use of machine learning to identify children with autism and their motor abnormalities. *Crippa, Salvatore et al. 2015, Journal of Autism and Developmental Disorders.*

ML models | Examples

	Overall mean	Optimal configuration
Diagnostic accuracy (sensitivity / specificity)	85 (82/ 89)%	97 (100/ 94)%

7 optimal features out of 17

sub-movement 2
the movement to transport the ball from a support to the target hole in which the ball was to be dropped

1. total movement duration
2. delta wrist angle
3. # movement units
4. time of peak deceleration
5. peak acceleration
6. time of peak velocity
7. peak velocity

Use of machine learning to identify children with autism and their motor abnormalities. *Crippa, Salvatore et al. 2015, Journal of Autism and Developmental Disorders.*

ML models | Examples

Attention-Deficit/Hyperactivity Disorder

ML models | Examples

Diagnosis of ADHD & Identification of a signature

22

TD

22

ADHD

A dataset of 44
school-aged children (~11 years old)

Multidomain profile of measures
. biological data
. neuropsychological data
. Near-InfraRed Spectroscopy (NIRS)

ADHD **Attention Deficit / Hyperactivity Disorder**
TD Typically-developing children

The Utility of a computerized algorithm Based on a Multi-Domain Profile of Measures for the Diagnosis of attention deficit/hyperactivity Disorder. *Crippa, Salvatore et al. 2017, Frontiers in Psychiatry.*

ML models | Examples

Multi-domain profile of measures

Biological data

10 features

Neuropsychological data

18 features

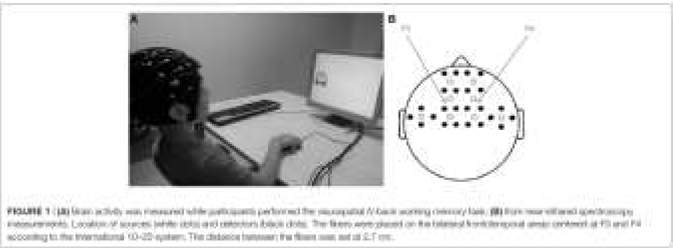

Near-InfraRed Spectroscopy (NIRS)

Oxy/Deoxy data from 32 channels

The Utility of a computerized algorithm Based on a Multi-Domain Profile of Measures for the Diagnosis of attention deficit/hyperactivity Disorder. *Crippa, Salvatore et al. 2017, Frontiers in Psychiatry.*

ML models | Examples

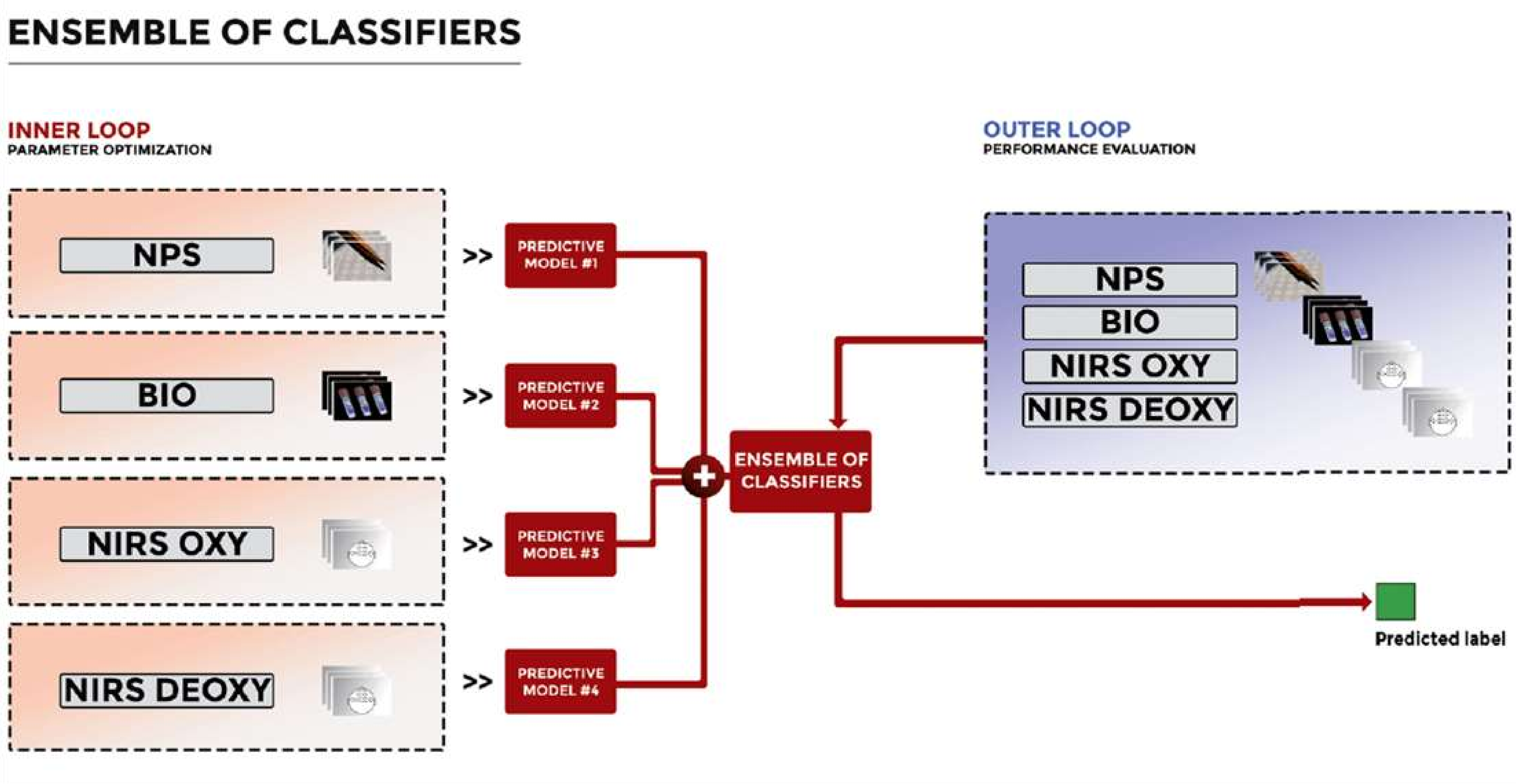

The Utility of a computerized algorithm Based on a Multi-Domain Profile of Measures for the Diagnosis of attention deficit/hyperactivity Disorder. *Crippa, Salvatore et al. 2017, Frontiers in Psychiatry.*

ML models | Examples

Measures	Accuracy (mean ± sd)	Sensitivity (mean ± sd)	Specificity (mean ± sd)
Neuropsychological	62 ± 17	70 ± 27	57 ± 24
Biological	66 ± 21	58 ± 40	73 ± 29
NIRS OXY	57 ± 27	48 ± 47	67 ± 33
NIRS DEOXY	78 ± 22	72 ± 34	82 ± 24
NIRS OXY + DEOXY	72 ± 32	73 ± 29	68 ± 43

biological features

.linoleic acid
.PUFA
.AA
.EPA
.omega-3 index
.AA/DHA
.AA/EPA
.MUFA

linoleic acid and total amount of polyunsaturated fatty acids

The Utility of a computerized algorithm Based on a Multi-Domain Profile of Measures for the Diagnosis of attention deficit/hyperactivity Disorder. *Crippa, Salvatore et al. 2017, Frontiers in Psychiatry.*

ML models | Examples

Measures	Accuracy (mean ± sd)	Sensitivity (mean ± sd)	Specificity (mean ± sd)
Neuropsychological	62 ± 17	70 ± 27	57 ± 24
Biological	66 ± 21	58 ± 40	73 ± 29
NIRS OXY	57 ± 27	48 ± 47	67 ± 33
NIRS DEOXY	78 ± 22	72 ± 34	82 ± 24
NIRS OXY + DEOXY	72 ± 32	73 ± 29	68 ± 43

neuropsychological features

.***sustained attention***-*false alarms*
.***visual set***-*shifting-RT inhibition*
.*sustained attention-coefficient of variation*
.*visual set-shifting-number of inhibition errors*
.***focused attention***-*RT correct responses*
.*focused attention-correct rejections target non-relevant position*
.*focused attention-SD of correct responses RT*
.*focused attention-misses*
...

measures of vigilance, focused and sustained attention, and cognitive flexibility

The Utility of a computerized algorithm Based on a Multi-Domain Profile of Measures for the Diagnosis of attention deficit/hyperactivity Disorder. *Crippa, Salvatore et al. 2017, Frontiers in Psychiatry.*

ML models | Examples

Single domain

Measures	Accuracy (mean ± sd)	Sensitivity (mean ± sd)	Specificity (mean ± sd)
Neuropsychological	62 ± 17	70 ± 27	57 ± 24
Biological	66 ± 21	58 ± 40	73 ± 29
NIRS OXY	57 ± 27	48 ± 47	67 ± 33
NIRS DEOXY	78 ± 22	72 ± 34	82 ± 24
NIRS OXY + DEOXY	72 ± 32	73 ± 29	68 ± 43

Multi-domain

Measures	Accuracy (mean ± sd)	Sensitivity (mean ± sd)	Specificity (mean ± sd)
NPS + BIO + NIRS OXY			
NPS + BIO + NIRS DEOXY			
NPS + NIRS OXY + NIRS DEOXY			
BIO + NIRS OXY + NIRS DEOXY			
NPS + BIO + NIRS OXY + NIRS DEOXY			

The Utility of a computerized algorithm Based on a Multi-Domain Profile of Measures for the Diagnosis of attention deficit/hyperactivity Disorder. *Crippa, Salvatore et al. 2017, Frontiers in Psychiatry.*

ML models | Examples

Single domain

Measures	Accuracy (mean ± sd)	Sensitivity (mean ± sd)	Specificity (mean ± sd)
Neuropsychological	62 ± 17	70 ± 27	57 ± 24
Biological	66 ± 21	58 ± 40	73 ± 29
NIRS OXY	57 ± 27	48 ± 47	67 ± 33
NIRS DEOXY	78 ± 22	72 ± 34	82 ± 24
NIRS OXY + DEOXY	72 ± 32	73 ± 29	68 ± 43

Multi-domain

Measures	Accuracy (mean ± sd)	Sensitivity (mean ± sd)	Specificity (mean ± sd)
NPS + BIO + NIRS OXY	71 ± 10	70 ± 27	73 ± 24
NPS + BIO + NIRS DEOXY	81 ± 15	73 ± 24	87 ± 22
NPS + NIRS OXY + NIRS DEOXY	78 ± 18	70 ± 36	87 ± 22
BIO + NIRS OXY + NIRS DEOXY	77 ± 21	63 ± 31	90 ± 21
NPS + BIO + NIRS OXY + NIRS DEOXY	76 ± 16	83 ± 22	68 ± 23

The Utility of a computerized algorithm Based on a Multi-Domain Profile of Measures for the Diagnosis of attention deficit/hyperactivity Disorder. *Crippa, Salvatore et al. 2017, Frontiers in Psychiatry.*